

## **General Disclaimer**

### **One or more of the Following Statements may affect this Document**

- This document has been reproduced from the best copy furnished by the organizational source. It is being released in the interest of making available as much information as possible.
- This document may contain data, which exceeds the sheet parameters. It was furnished in this condition by the organizational source and is the best copy available.
- This document may contain tone-on-tone or color graphs, charts and/or pictures, which have been reproduced in black and white.
- This document is paginated as submitted by the original source.
- Portions of this document are not fully legible due to the historical nature of some of the material. However, it is the best reproduction available from the original submission.

**FINAL REPORT**

**July, 1977**

**ANALYSIS OF RESULTS OF ASTP EXPERIMENT IN ELECTROPHORESIS**

**NAS8-32124**

**Prepared for**

**National Aeronautics and Space Administration  
George C. Marshall Space Flight Center  
Marshall Space Flight Center, Alabama 35812**

**Prepared by**

**Principal Investigator: J. W. Vanderhoff**

**Co-Investigator: F. J. Micale**

**Research Assistant: P. H. Krumrine**

**Lehigh University**

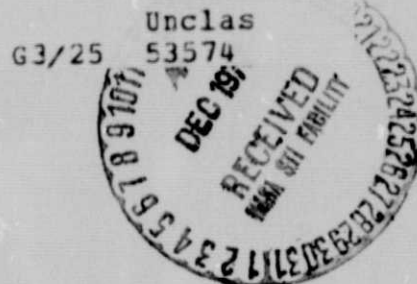
**Center for Surface and Coatings Research**

**Sinclair Laboratory, Bldg. #7**

**Bethlehem, Pennsylvania 18015**

(NASA-CR-150469) ANALYSIS OF RESULTS OF  
ASTP EXPERIMENT IN ELECTROPHORESIS Final  
Report (Lehigh Univ.) 43 FFC A03/MF A01  
CSCI 07D

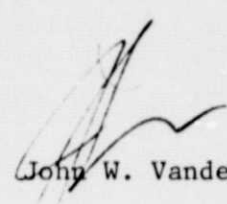
**N78-12168**




Addendum to Final Report "Analysis of Results of ASTP Experiment in Electrophoresis", NASS-32124, July 1977.

The MA-011 electrophoretic separation of human kidney cells prepared by G. Barlow (Abbott Laboratories) was not analyzed using the theoretical model described in this report, although the Work Statement of this project stated that this analysis would be carried out. In the event, however, this proved impossible. The kidney cell separation was carried out in a covered channel so that the separation could not be photographed; no flight films were available, as was the case for the human-rabbit-horse fixed red blood cell mixture. Even so, the separation could be predicted from the original electrophoretic mobility distribution and compared with the number of cells found in each fraction obtained by slicing the frozen specimen after return to earth. This also was not possible, because the electrophoretic mobility distribution of the sample submitted for separation was not measured beforehand, and the results for the sliced fractions were reported in terms of the number of viable cells and their rate of urokinase production, instead of the total number of cells. Therefore, there was no basis for calculation and no basis for comparison of the calculated results.

To predict electrophoretic separations using the mathematical model described in this report requires the initial distribution of electrophoretic mobilities of the sample, the dimensions of the electrophoresis channel, and the conditions of the experiment.

  
John W. Vanderhoff

  
F. J. Micale



## TABLE OF CONTENTS

|   | Page |
|---|------|
| Introduction . . . . .                  | 1    |
| Experimental . . . . .                  | 2    |
| Theoretical Computer Modeling . . . . . | 5    |
| Photographic Analysis . . . . .         | 13   |
| Conclusions . . . . .                   | 25   |



## LIST OF FIGURES

|   | Page |
|---|------|
| Figure 1. Electrophoretic mobility distribution of rabbit, human and horse fixed red blood cells  | 4    |
| Figure 2. Computer electrophoretic mobility distributions of fixed red blood cells  | 7    |
| Figure 3. Effect of electroosmosis on cell separation with $T=2^{\circ}\text{C}$ , $R=0.75$ and $\Theta=0.3\text{cm}$ .   | 9    |
| Figure 4. Effect of temperature gradient, $T$ , on cell separation with $U_{OS} = -0.2 \text{ cm/volt sec.}$ , $R = 0.75$ and $\Theta = 0.3 \text{ cm}$ .   | 10   |
| Figure 5. Effect of ratio of sample plug radius to channel radius, $R$ , on cell separation with $U_{OS} = -0.2 \text{ um cm/volt sec}$ , $T = 2^{\circ}\text{C}$ and $\Theta = 0.3 \text{ cm}$ . | 11   |
| Figure 6. Effect of sample plug thickness, $\Theta$ , on cell separation with $U_{OS} = -0.2 \text{ um cm/volt sec}$ , $T = 2^{\circ}\text{C}$ and $R = 0.75$ .                                   | 12   |
| Figure 7. Band displacements as a function of time in Column 1.   | 14   |
| Figure 8. Band displacements as a function of time in Column 5.   | 16   |
| Figure 9. Position of bands as determined from visual observation of flight film and theory.  | 17   |
| Figure 10. Micro-densitometer scan and computed displacement.<br>A. Raw data micro-densitometer scan for Frames 1 and 10.<br>B. Net micro-densitometer scan and computed displacement.            | 19   |
| Figure 11. Micro-densitometer scan and computed displacement.<br>A. Frame 4, 12 minutes separation.<br>B. Frame 6, 18 minutes separation.   | 20   |
| Figure 12. Micro-densitometer scan and computed displacement.<br>A. Frame 8, 24 minutes separation.<br>B. Frame 10, 30 minutes separation.  | 21   |
| Figure 13. Micro-densitometer scan and computed displacement.<br>A. Frame 12, 36 minutes separation.<br>B. Frame 14, 42 minutes separation.   | 22   |

LIST OF FIGURES (continued)

|   | Page |
|---|------|
| Figure 14. Micro-densitometer scan and computed displacement. |      |
| A. Frame 16, 48 minutes separation.                           |      |
| B. Frame 16, 52 minutes separation.                           | 23   |
| Figure 15. Micro-densitometer scan and computed displacement. |      |
| A. Frame 20, 60 minutes separation.                           |      |
| B. Frame 22, 66 minutes separation.                           | 24   |

This report was prepared by Lehigh University under NAS8-32124 "Analysis of Results of ASTP Experiment in Electrophoresis" for the George C. Marshall Space Flight Center of the National Aeronautics and Space Administration.

### Introduction

The Apollo-Soyuz Test Project (ASTP) carried out in July, 1975 included an electrophoretic separation experiment of biological cells (MA-011). The nature of these experiments was to determine if biological separations could be carried out in space under microgravity conditions and with better resolution than obtainable on earth. The experiments consisted of a series of static and isotachoelectrophoresis experiments in which mixtures of aldehyde-fixed red blood cells, B and T lymphocytes, and urokinase producing kidney cells were separated. The separation results of the aldehyde-fixed rabbit, human and horse red blood cells, which were taken in the form of photographs taken at three-minute intervals in columns 1 and 5, are the subject of this report.

Previously, static electrophoresis experiments had been carried out on Apollo 14 with a mixture of colored dyes (1), and on Apollo 16 with a mixture of two monodisperse polystyrene latexes (2,3), but the resolution of these experiments was poor due to the electroosmotic effect on the fluid velocity. With the development of a suitable coating, the electroosmosis could be considerably reduced, and the ASTP electrophoresis experiments would justify and provide valuable information for further experiments to be carried out on the space shuttle and future programs.

There are various advantages to performing such experiments in space under microgravity conditions. The primary advantage is the elimination of the thermal convection mixing due to Joule heating of the liquid. In a gravity environment this fluid mixing due to density gradients obviates any possible separation. To perform a similar experiment on earth, a much lower voltage would be required

resulting in less Joule heating, but also a much slower separation and longer separation time, leading to further problems. As the separation time increases, diffusion due to Brownian motion increases, thus decreasing the resolution. A second advantage is the elimination of particle sedimentation due to a density differential between the suspending fluid and the particles. If the particles settle the bands will become distorted decreasing the resolution. Therefore, these two advantages lead to a much improved separation resolution than is possible on earth. The obvious disadvantages are cost, scheduling limitations, and only small quantities may be sent and returned.

### Experimental

The development of a low electroosmotic mobility coating greatly improved the resolution of the electrophoretic separations. A complete description of the coating development and theory may be found in previous work (4,5), so only a brief discussion will follow. The coating for glass channels consisted of a precoat of Dow Corning Z6040,  $\gamma$ -glycidoxypropyltrimethoxysilane, which bound the methylcellulose to the glass surface. The surface was then repeatedly washed or rinsed to remove unbound methylcellulose. Such a coating generally reduced the value of electroosmosis from values of  $-4.00$  to  $-0.20 \mu\text{m cm/volt sec}$ . This reduction in electroosmosis results in sample migration by bands rather than elongated cones which can't be resolved. Therefore, this coating played a significant role in improving the results and resolution for the ASTP electrophoresis experiments.

Many species of fixed red blood cells were considered as candidates for the space experiment. Among these were chicken, dog, horse, human, turkey, cow, pig and rabbit red blood cells fixed with both formaldehyde and glutaraldehyde solutions. The species finally chosen to give the broadest range of electrophoretic mobilities and the best chance of separating were horse, human, and rabbit fixed red blood cells. Mobility distributions were determined by microcapillary electrophoresis

techniques and are shown for the three candidate species in Figure 1. Measurements were done by both Dr. Robert Knox of the University of Oregon (6) and ourselves and are displayed on the graph in two forms. The data of Dr. Knox is represented in bar graph form and represents 100 measurements per each cell species with the area under each curve proportional to the relative concentrations of the space samples. Our data is presented in a smoothed form and represents 150 measurements per each cell species. The measurements were performed in the A-1 buffer formulated for these experiments and agree well with respect to average mobility and range for each cell type.

The basic procedure for the electrophoresis experiments entailed the preparation of the columns and sample slides on earth. Each column was thoroughly cleaned then coated with the Z6040-MC coating and rinsed for three days, after which they were separately sealed in plastic bags and stored for travel into space. The red blood cells were aldehyde fixed and measured for electrophoretic mobility. A mixture of 32.8% rabbit, 21.6% human, and 45.6% horse cells with a total concentration of  $2.52 \times 10^7$  red blood cells per slide was prepared by freezing the cells in a small disc shape, 0.478 cm in diameter by 0.312 cm thick. These sample discs were then placed in a freezer for storage until time for the experiment. All electrophoresis experiments were done in duplicate on two separate days. Columns preloaded with A-1 buffer were placed in the apparatus. A sample disc was removed and inserted into one end of the column and allowed to thaw and the current turned on. The samples were allowed to electrophoresis for about 60 minutes with photographs taken every 3 minutes to record data. After 60 minutes the current was turned off and the freezing cycle begun. The frozen columns were then removed and placed in storage for return to earth for further analysis. Postflight analysis consisted of removing the frozen core from each column and slicing it into 5 mm. slices which were analyzed for red blood cell count and mobility.

Two problems occurred which marred the experiment and collection of important data. First, column 5 probably developed an air bubble which migrated to

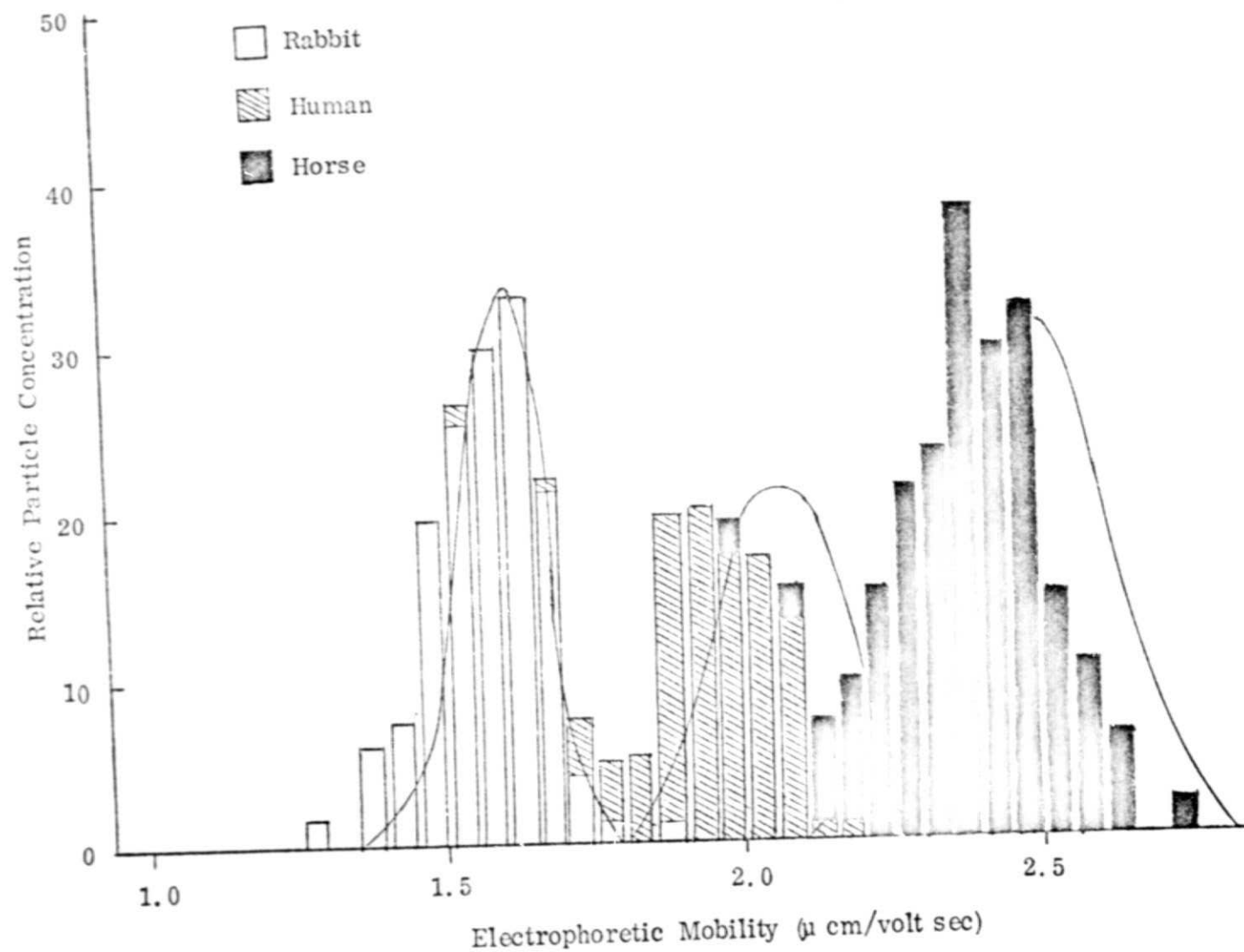


Figure 1. Electrophoretic mobility distribution of rabbit, human and horse fixed red blood cells.



the far electrode causing the voltage to saturate. For this reason, the voltage was turned off temporarily and restarted but migration did not proceed down the entire column and some swirling was observed. The second problem occurred in the postflight slicing of column 1. Upon removal of the core, it broke and only very large slices were able to be made, which reduced the amount of information obtainable. As luck would have it, this was the column that performed well in space which should have provided the best information. Therefore, only a fraction of the data was obtained, from which conclusions could be drawn as to the degree of success. Further information and analysis was extracted from the photographs which will be covered in detail later in this report.

### Theoretical Computer Modeling

A large amount of effort was expended in developing a theoretical computer model of a static electrophoresis column (4, 7). With such a model many parameters can be varied very easily to determine the specific effect of each one, and this information can then lead to a better design or choice of operating conditions by which the resolution can be maximized. Also, before an experiment is performed, the model can be used to predict separations, or afterwards to compare results to theory. Therefore, the development of such a model is very useful as an analytical tool in studying static electrophoresis.

The model which has been used is rather simple in that it only accounts for effects on a macroscopic scale, ignoring particle interactions, diffusion, relaxation effects, and electric field distortion effects on individual particles. Of prime interest is the displacement and distortion of each particle band and the relative particle concentration along the column axis. This information is best expressed with the equation:

$$d = \left[ U_e E \frac{\epsilon_2 \eta_{298}}{\eta_2 \epsilon_{298}} - U_{os} E \frac{\epsilon_1 \eta_{298}}{\eta_1 \epsilon_{298}} \left( \frac{r^2}{a^2} - 1 \right) \right] t \quad (1)$$

where  $d$  = displacement distance ( $\mu\text{m}$ )

$U_e$  = electrophoretic mobility ( $\mu\text{m cm/volt sec}$ )

$U_{os}$  = electroosmotic mobility ( $\mu\text{m cm/volt sec}$ )

$r$  = radial distance ( $\text{cm}$ )

$a$  = channel radius ( $\text{cm}$ )

$E$  = applied potential gradient ( $\text{volts/cm}$ )

$t$  = time ( $\text{sec}$ )

$\epsilon$  = dielectric constant of suspending fluid -  $f(T)$

$\eta$  = viscosity of suspending fluid -  $f(T)$

The subscripts 1, 2, and 3 refer to temperatures at the wall, at a distance  $r$ , and at the center respectively, while 298 refers to the reference temperature in degrees Kelvin at which the electrophoretic and electroosmotic mobilities were measured. Equation 1 describes the displacement of a discrete element as a function of radial position in the channel. It also shows that the radial dependence can be reduced but not eliminated if the electroosmotic mobility is reduced to zero since the second term then becomes zero and the first term is a function of  $r$  through  $\epsilon_2$  and  $\eta_2$ .

Equation 1 may be used to define the band shape and particle concentration for each species as a function of time. First, a least squares algorithm is used to fit a smoothed curve of up to a fifth order polynomial through a set of points from the bar graph mobility distribution of each particle species. These computed mobility distributions are shown in Figure 2 where the area under the curves is proportional to the actual concentration of cells. Next, the initial sample disc is divided up into a series of small finite elements, and Equation 1 is applied to each element as a function of radial position. Each element is assumed to have the same mobility distribution which is used to determine the spread and concentration profile for each element. Then the contribution from each element is summed up to determine the total concentration profile for each species and the band as a whole. With a computer, this summing process can be done very quickly and accurately for a large number of elements so as to allow a very high degree of confidence in the results. This is



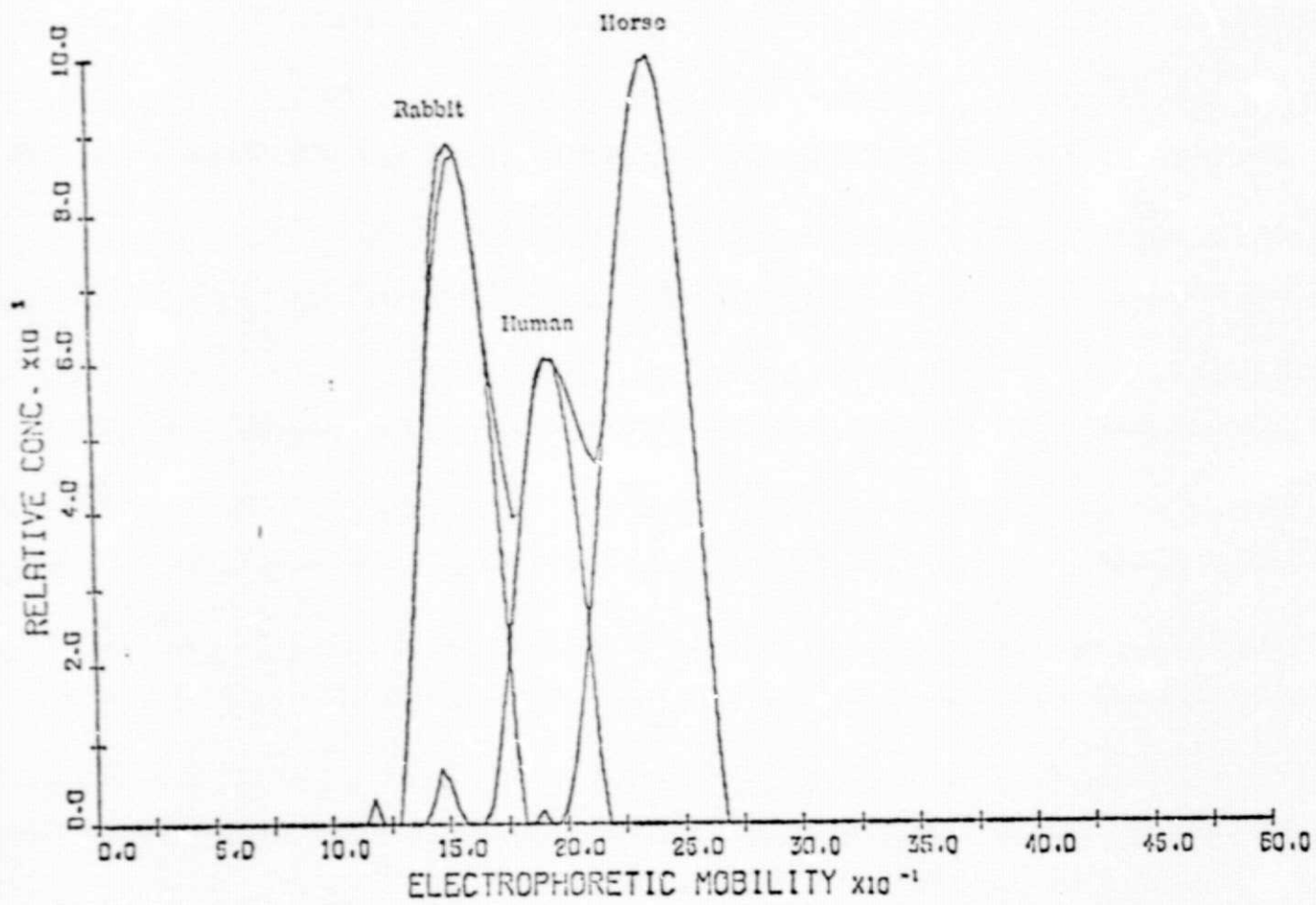


Figure 2. Computer electrophoretic mobility distributions of fixed red blood cells.

essentially how the computerized model was constructed so as to allow determination of band displacement, shape, and concentration for species exhibiting a broad mobility distribution. It could also be used to determine where each mobility fraction from a bar graph should be found. A listing of the actual program may be found in Appendix A.

With the help of this program, it was then possible to compare the theoretical resolution for a number of experimental conditions using the mobility distribution and relative concentration of the fixed red blood cells used for the space experiment where the location of the cells, from left to right, are always rabbit, human and horse. Figures 3 through 6 show the predicted separations and the effects of four important parameters on the resolution. In each figure, one parameter is compared at three values maintaining all other conditions constant, and the separation time is 60 minutes. The central figure in each case corresponds most closely to the actual experimental conditions used on ASTP and is, therefore, the same in all four figures. Figure 3 shows the effect of electroosmosis,  $U_{os}$ , on resolution for values of -0.40, -0.20 and 0.00  $\mu\text{m cm/volt sec}$ . It is readily apparent that this parameter can have a profound effect on the resolution, with best results expected for values as close to zero as possible. It should be noted that even for a value of 0.00  $\mu\text{m cm/volt sec}$ , there is still some curvature to the band boundaries and this results from the  $2^\circ\text{C}$  temperature gradient predicted from Joule heating in the channel. Temperature is important because both dielectric constant and viscosity are functions of temperature and affect electrophoretic and electroosmotic mobility. Figure 4 shows the effect when this temperature gradient,  $\Delta T$ , is the variable. The three cases correspond to gradients of  $10^\circ\text{C}$ ,  $2^\circ\text{C}$  and  $-6^\circ\text{C}$  from channel center to channel wall. Obviously if it were possible to maintain the center at a cooler temperature than the walls, then conditions would be improved, but such a condition is physically impossible for this system where Joule heating predominates. Figure 5 shows the effect of decreasing the ratio of sample plug radius to the channel radius,  $R$ , for values of 1.00, 0.75, and 0.50. Smaller values of this ratio can improve the

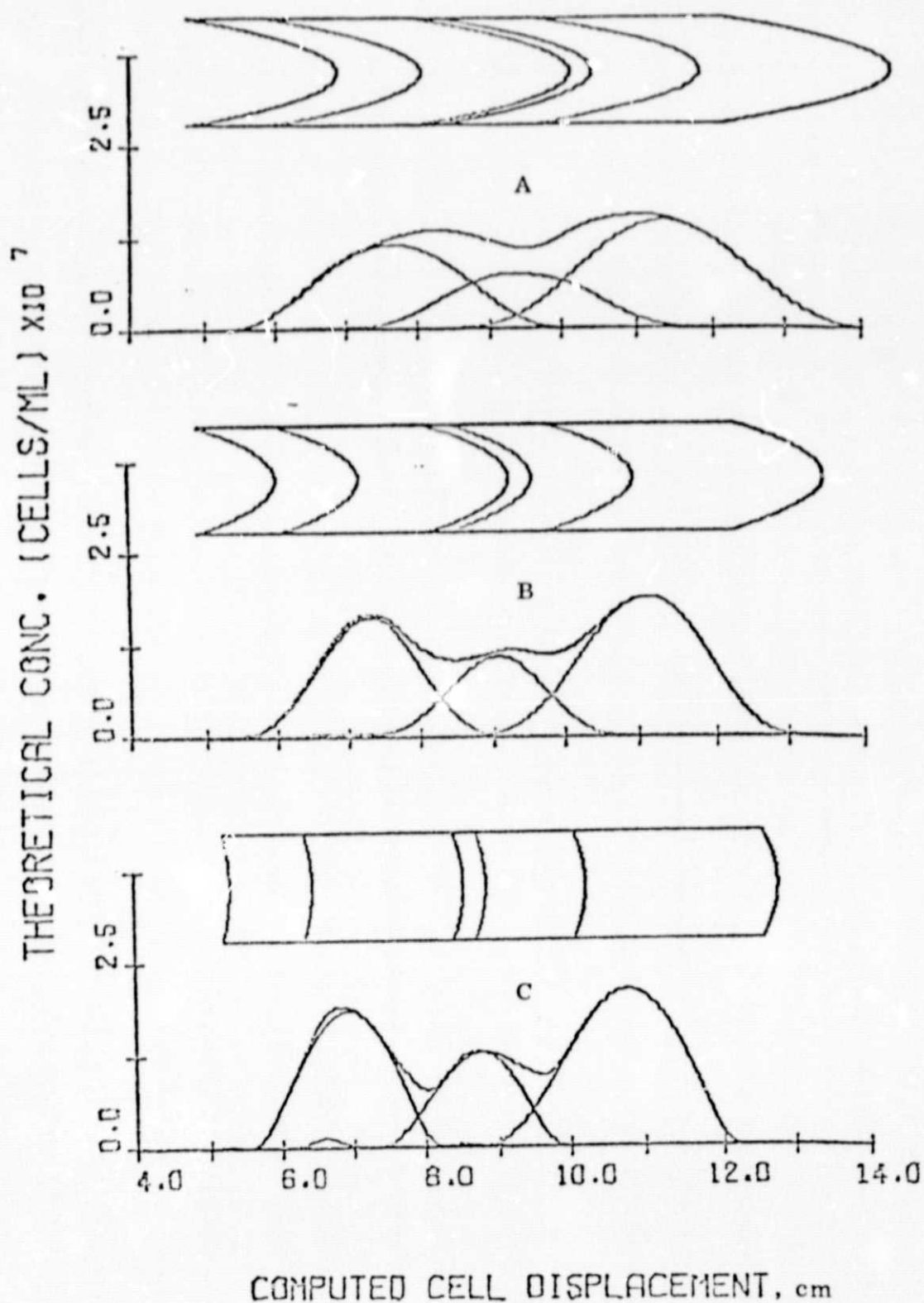
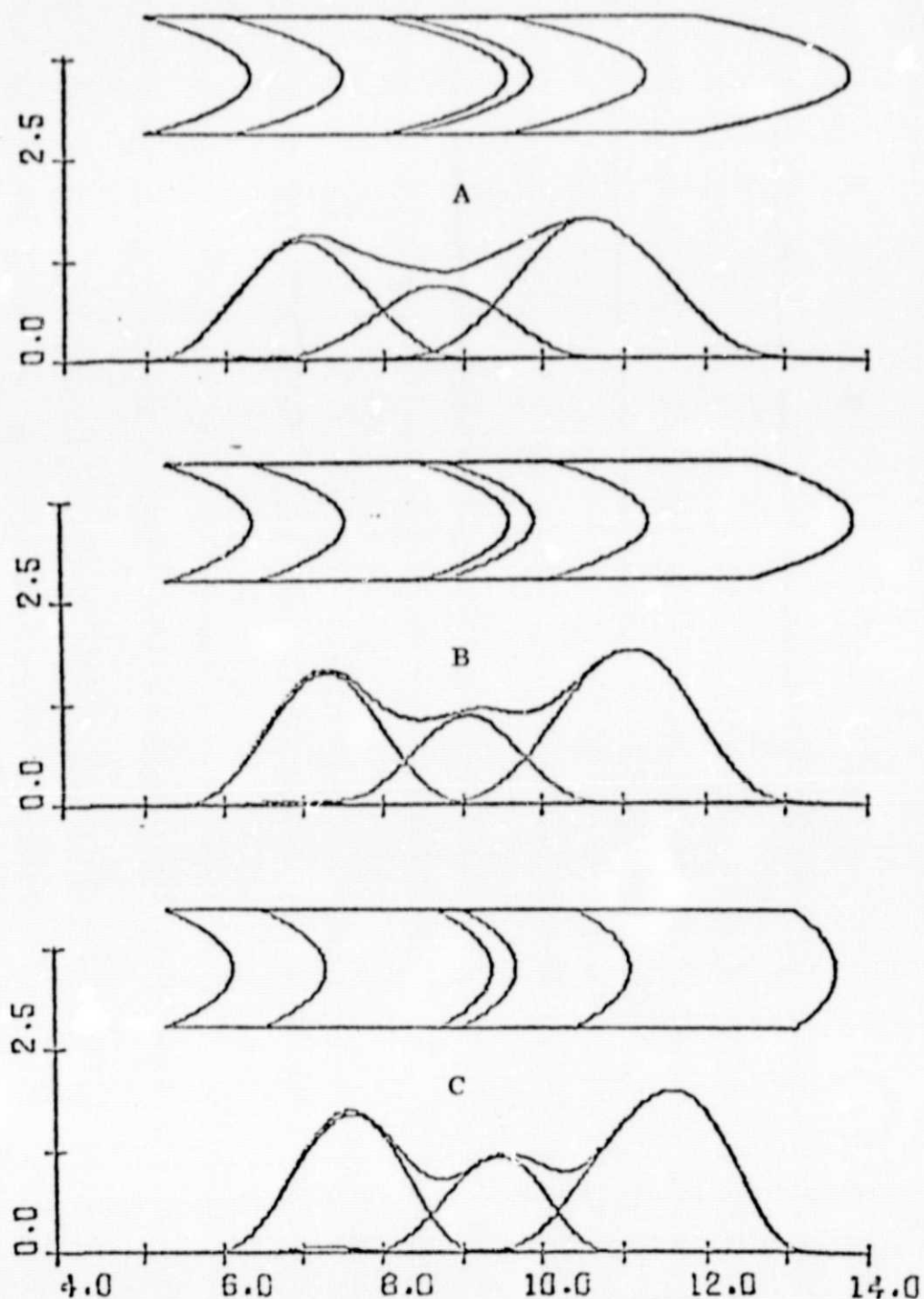


Figure 3. Effect of electroosmosis on cell separation with  $\Delta T = 2^\circ \text{C}$ ,  $R = 0.75$  and  $\Theta = 0.3 \text{ cm}$ . A,  $U_{os} = -0.4 \mu\text{m cm/volt sec}$ ; B,  $U_{os} = -0.2 \mu\text{m cm/volt sec}$ ; C,  $U_{os} = 0.0 \mu\text{m cm/volt sec}$ .

THEORETICAL CONC. (CELLS/ML)  $\times 10^7$



COMPUTED CELL DISPLACEMENT, cm

Figure 4. Effect of temperature gradient,  $\Delta T$ , on cell separation with  $U_{OS} = -0.2 \mu\text{m cm/volt sec.}$ ,  $R = 0.75$  and  $\Theta = 0.3 \text{ cm}$ ; A,  $\Delta T = 10^\circ\text{C}$ ; B,  $\Delta T = 2^\circ\text{C}$ ; C,  $\Delta T = -6^\circ\text{C}$ .

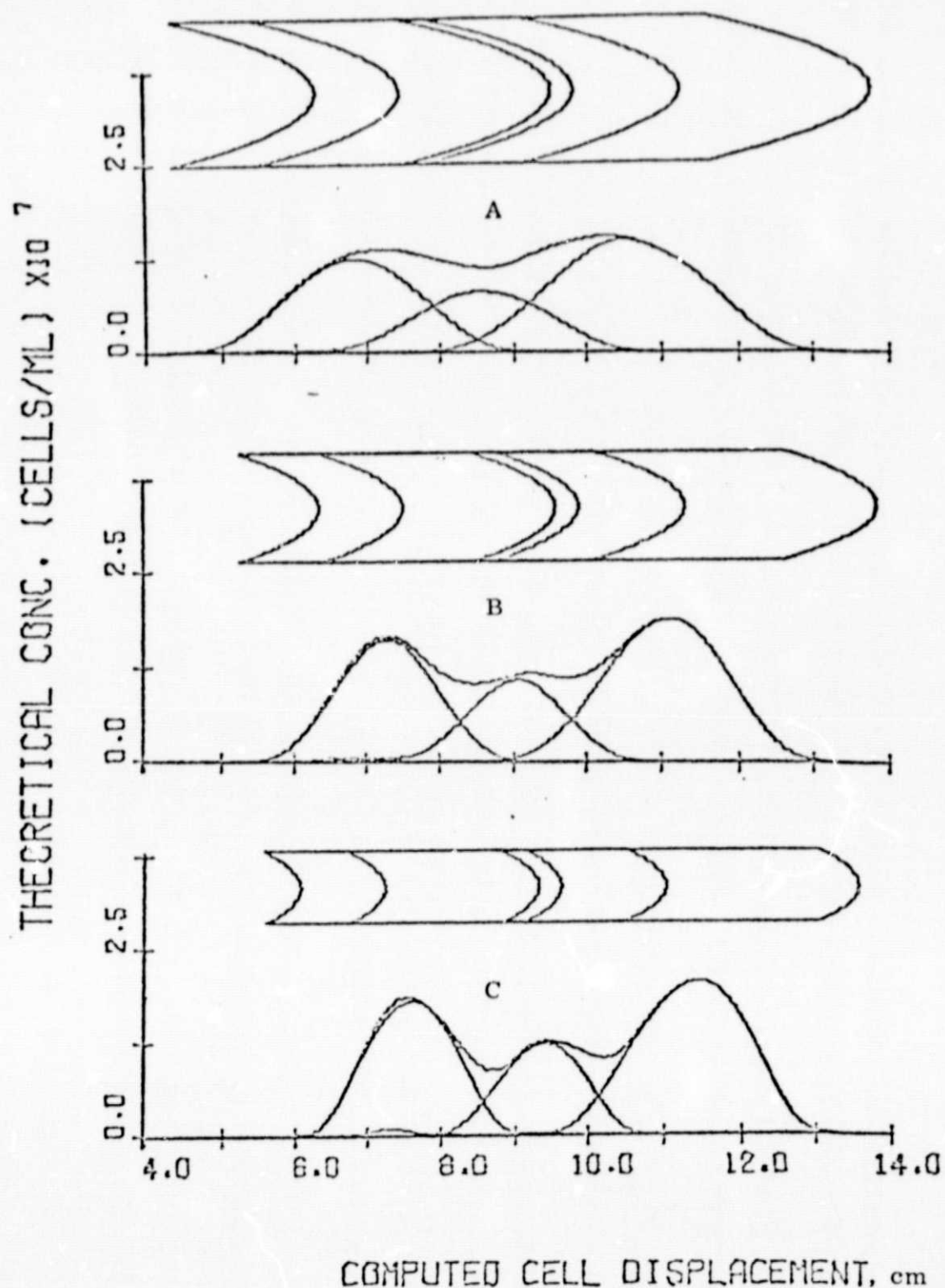


Figure 5. Effect of ratio of sample plug radius to channel radius,  $R$ , on cell separation with  $U_{OS} = -0.2 \mu\text{m cm/volt sec}$ ,  $\Delta T = 2^\circ\text{C}$  and  $\Theta = 0.3 \text{ cm}$ ; A,  $R = 1.0$ ; B,  $R = 0.75$ ; and C,  $R = 0.50$ .

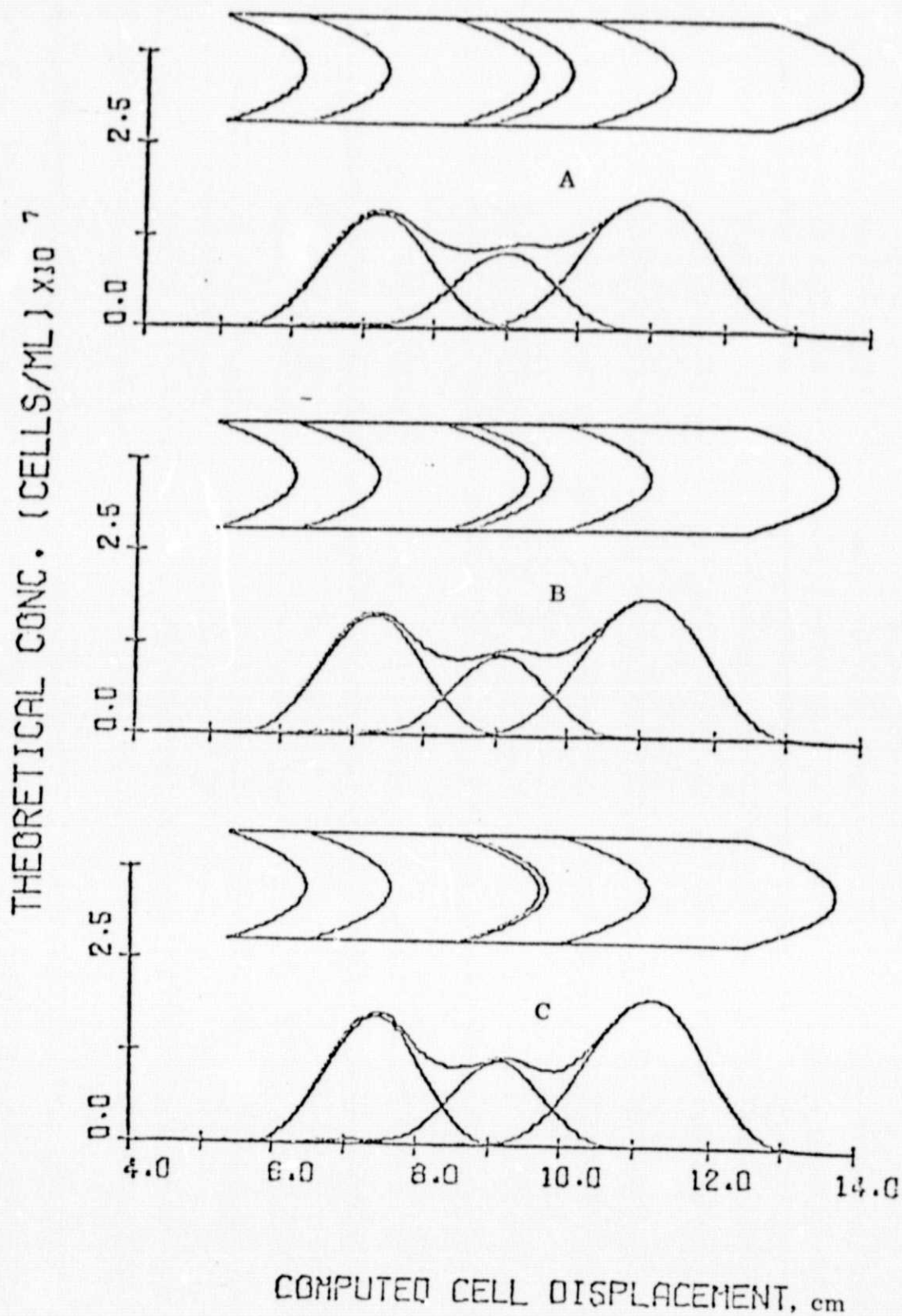


Figure 6. Effect of sample plug thickness,  $\Theta$ , on cell separation with  $U_{OS} = -0.2 \mu\text{m cm/volt sec}$ ,  $\Delta T = 2^\circ\text{C}$  and  $R = 0.75$ ; A,  $\Theta = 0.5 \text{ cm}$ ; B,  $\Theta = 0.3 \text{ cm}$ ; and C,  $\Theta = 0.1 \text{ cm}$ .



resolution especially if  $U_{os}$  is high, but at a cost of less sample volume which might be more important. Another factor effecting the volume is the initial sample plug thickness,  $\Theta$ , and this effect is shown in Figure 6. This parameter, for values of 0.5, 0.3 and 0.1 cm, is found to have only a small effect on the resolution, but this is because the migration distance is large in relation to  $\Theta$ , making it negligible. For cases with a large migration distance,  $R$  could be reduced and  $\Theta$  increased to maintain the desired volume but with improved resolution. It should be noted that even under optimum conditions, these particles could not be completely resolved into separate fractions because the mobility distributions overlap; however, they could be resolved according to their mobilities.

#### Photographic Analysis

As mentioned before, photographs were taken at 3 minute intervals, providing a pictorial account of the progress of the experiments. These photographs were able to provide valuable information as to the success of the low electroosmotic coating, validity of the theory and the results of the separation.

Initially, only the second generation film was available for observation and, therefore, only information on the apparent band boundaries could be extracted by visual examination. Figures 7 and 8 show the discernible boundaries and displacements versus time for the two columns containing fixed red blood cells. Of course, the exactness of these measurements depends entirely on the photographic quality and the judgement of the observer, but they are representative of the separation that took place. Figure 7 shows the results from Column #1, in which two bands were clearly discernible as the experiment progressed. At first, only one band of a lighter and darker region followed by another lighter region was visible. Then, at about 25 minutes into the experiment, the leading lighter region appeared to separate from the main portion as a separate band with apparently few fixed red blood cells in between. At about 42 minutes, the darker and lighter regions of the second band were no longer discernible. This data shows that the migration

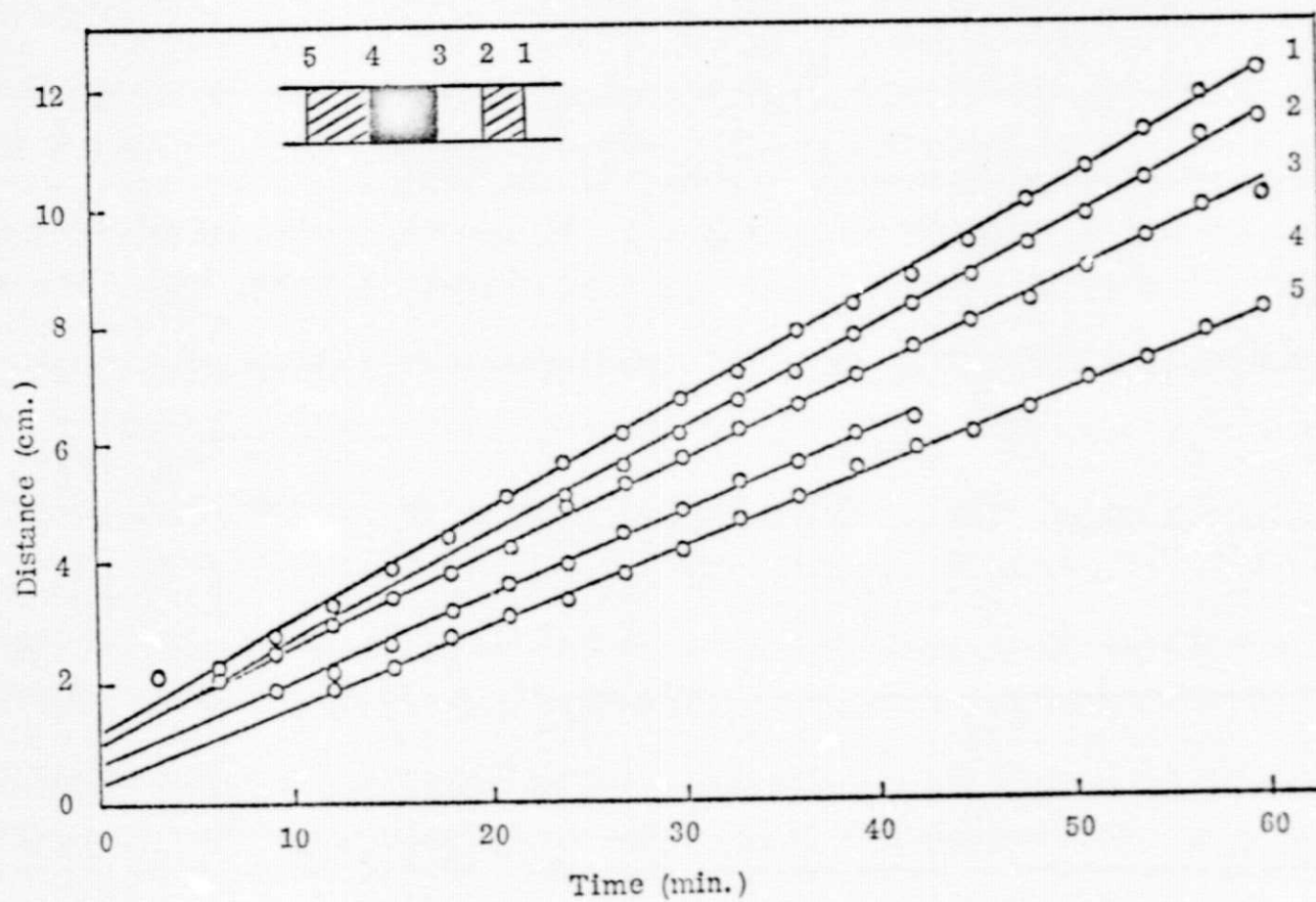


Figure 7. Band displacements as a function of time in Column 1.



of the band boundaries with respect to time proceeded at a linear rate which is as expected, and the rate corresponds to the mobility values that were determined for the fixed red blood cells and the electroosmosis with an applied gradient of 10.6 volts/cm. Also, the sharp planar boundaries attest to the low value of electroosmosis due to the methylcellulose coating. However, it seemed distressing that very few blood cells could be detected in the region between the two bands when the mobility distributions of the three species clearly overlapped. It could be possible that the concentration was low enough that it would not appear on the second generation film.

Figure 8 shows the results from Column #5 which incurred technical problems when an air bubble resulting from a leak migrated to the far electrode and probably caused the voltage to saturate. Some information may still be obtained from the two regions in which the migration proceeded normally. As in Column #1, there was a lighter and darker region as the bands emerged from the column end. Also the migration rate of the bands seemed to be very close to that in Column #1, confirming those results.

In an effort to compare these photographic results to the theoretical concentration, the computer was supplied with the best known values for all the parameters and allowed to compute the expected concentration profile which was divided up into four concentration regions. These results are shown in Figure 9 along with the experimental band appearances for Column #1. The experimental and theoretical concentrations are shown every six minutes versus migration distance. What this shows is that the fixed red blood cells should have been observed over a much larger portion of the column and in between the two bands. However, the agreement is acceptable, assuming that the concentration of cells was not sufficient to show up on the second generation film. There does seem to be some disagreement between experimental and theoretical in the displacement of the second band. This could be explained if there was some clumping of the cells due to the freezing and thawing process on such a high concentration of fixed red blood cells.

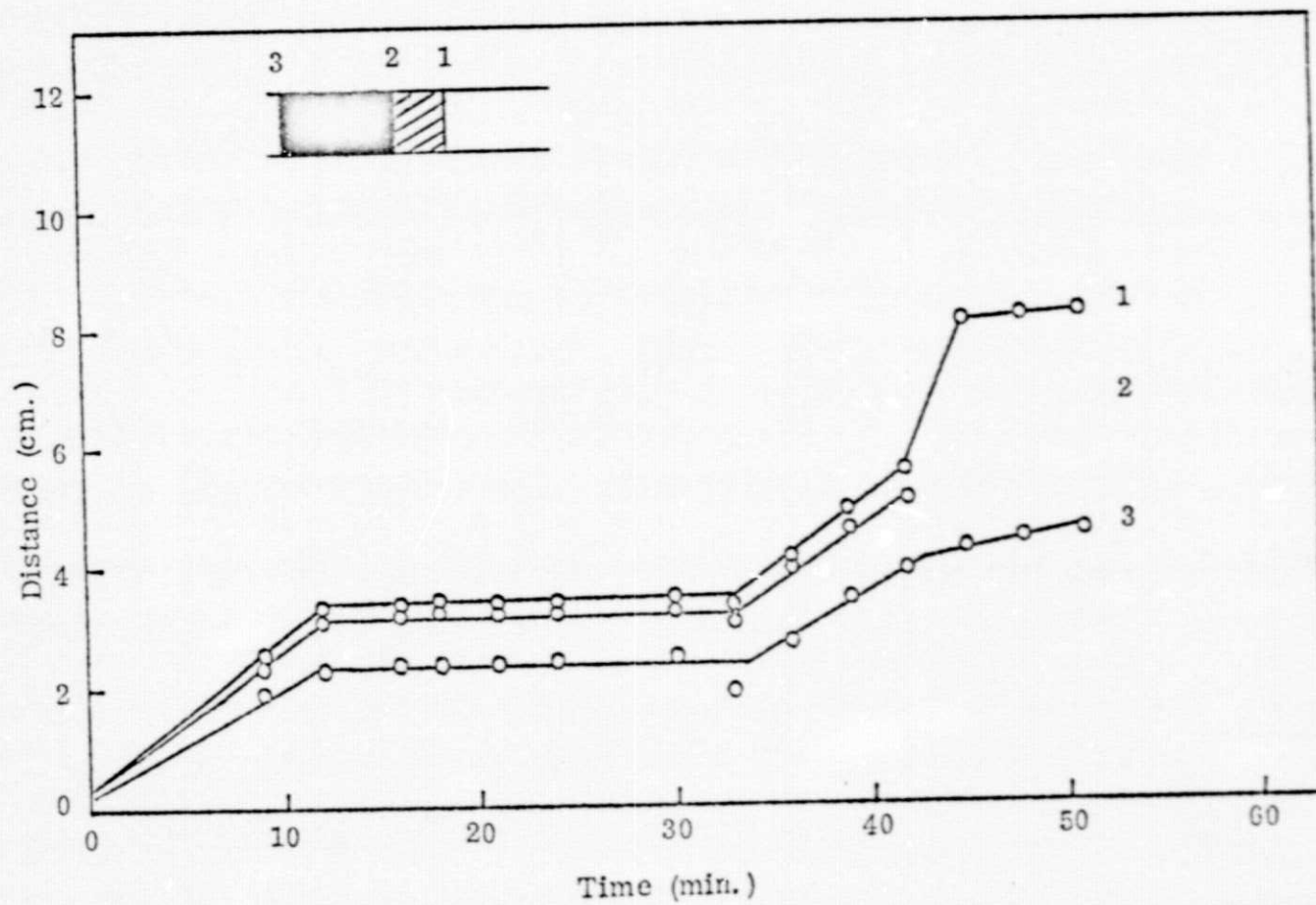


Figure 8. Band displacements as a function of time in Column 5.

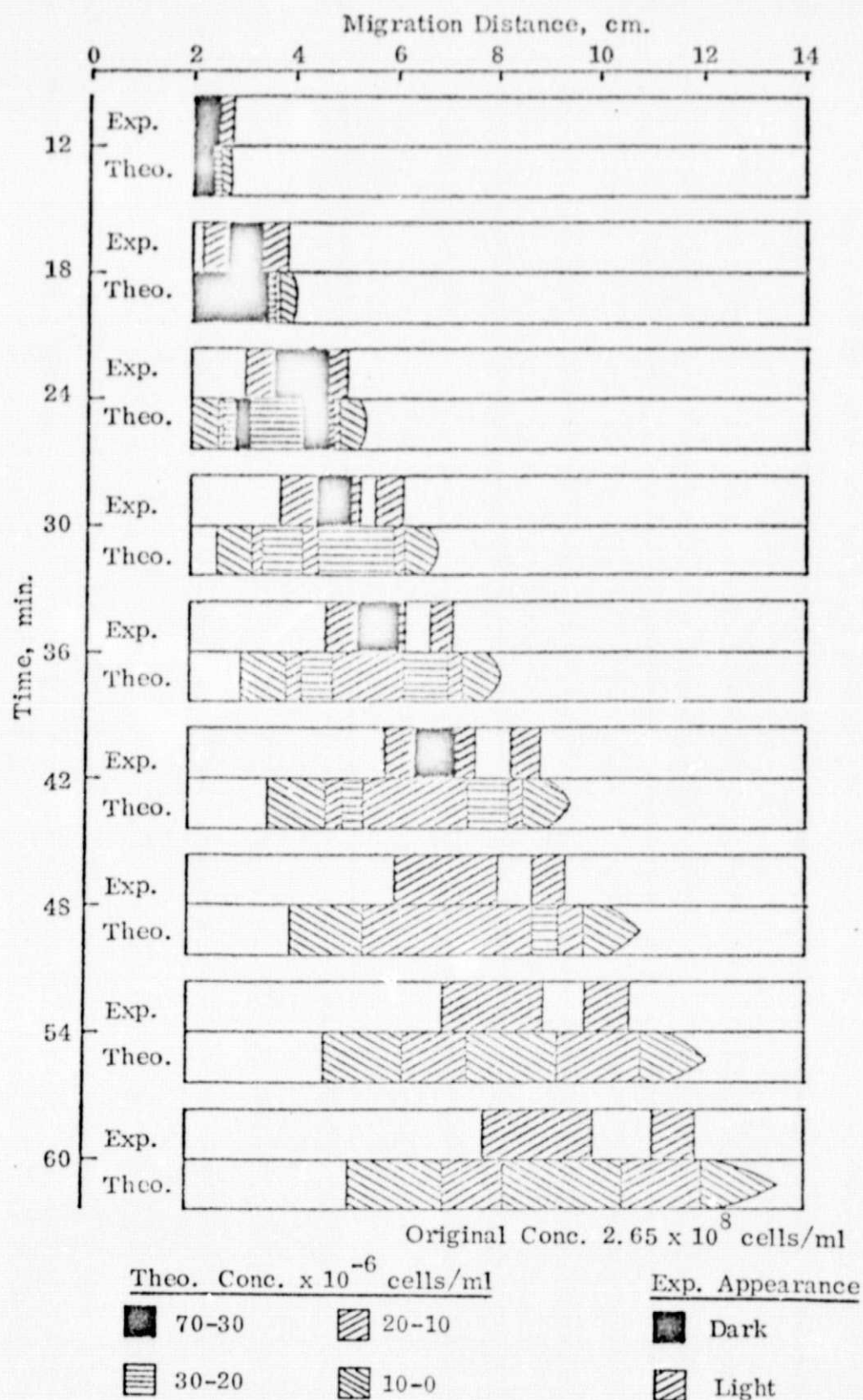


Figure 9. Position of bands as determined from visual observation of flight film and theory.

More recently, micro-densitometer scans of the first generation film, which shows much more detail, have been provided by NASA. The scans were taken by measuring the optical density of the separation column while traversing from one end of the column to the other end with a very small orifice in the direction of the traverse. Figure 10 shows two graphs obtained by this technique. Figure 10A shows a reproduction of scans obtained from frame 1 and frame 10, in which frame 1 is used as a base line with no cells yet present in the column. It should be noted that the two traces agree quite closely with only a small deviation in the background at distance greater than 8 cm. This is because the cells in frame 10, or 30 minutes into the separation, have not yet proceeded beyond this distance. The large deflection at about 7.5 cm is from the thermocouple present in the column at that position for monitoring temperature. Figure 10B shows two curves, one of the subtracted difference between the micro-densitometer scans corresponding to the left hand axis and the second of the computed cell concentration as evaluated from the theoretical model corresponding to the right hand axis. The theoretical model for these computations assumes an applied potential gradient of 10.6 volt/sec and  $U_{os}$  of  $-0.2 \mu\text{m/cm/volt sec}$ . Both the micro-densitometer and theoretical curves are generated by the computer and the areas under each curve equated for comparison.

Figures 11 through 15 show the results at six minute intervals or every second frame from 4 through 22. The theoretical results indicate the presence of two peaks as early as twelve minutes into the separation whereas the micro-densitometer results show the initiation of two peaks in frame 8 or 24 minutes into the separation. The breaking up of the band into two bands by visual observation of the flight film, Figure 9, occurs after 30 minutes of separation, frame 10. The micro-densitometer results, however, show that although the advancing peak increases in definition, it does not split off from the main band, Figures 12 through 15. Furthermore, while the position of the band, as it proceeds through the separation, agrees extremely well with the theoretical prediction, the magnitude and position of the second peak does not agree with theory. This discrepancy in band shape can be attributed to a number of reasons,

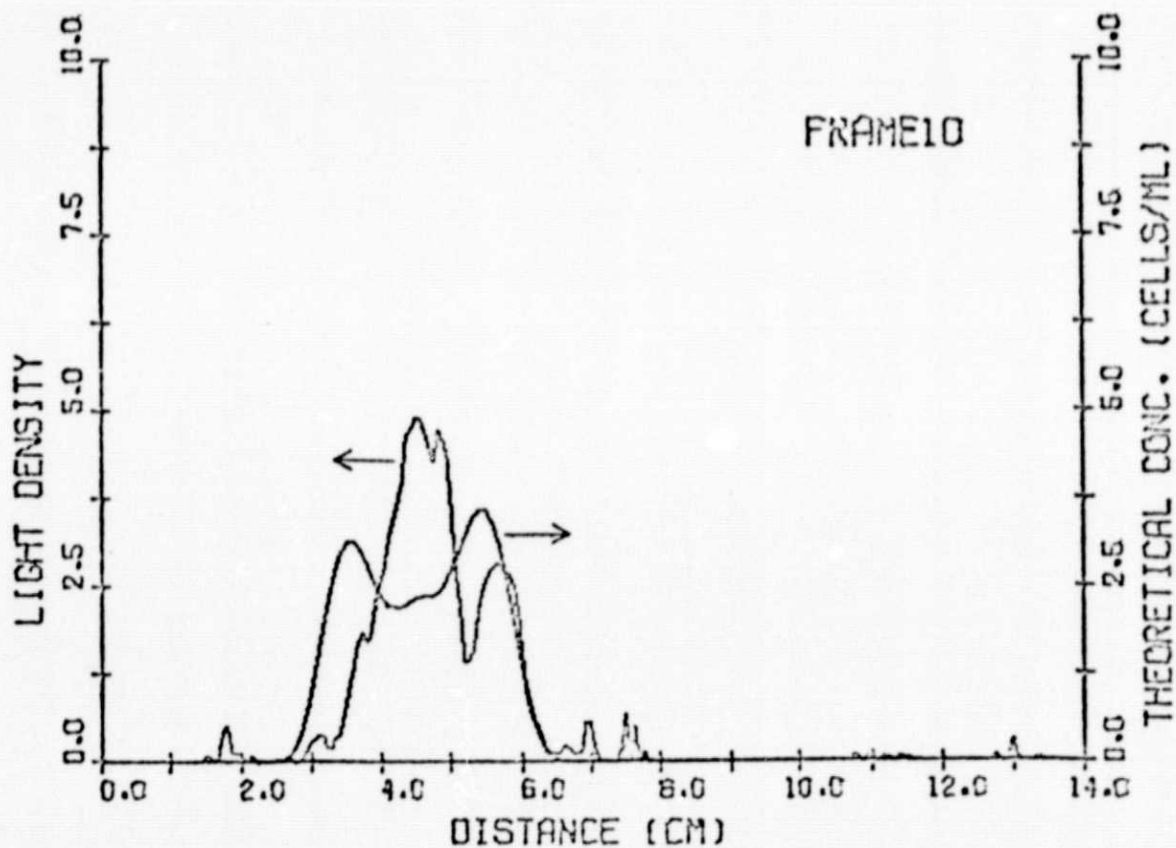
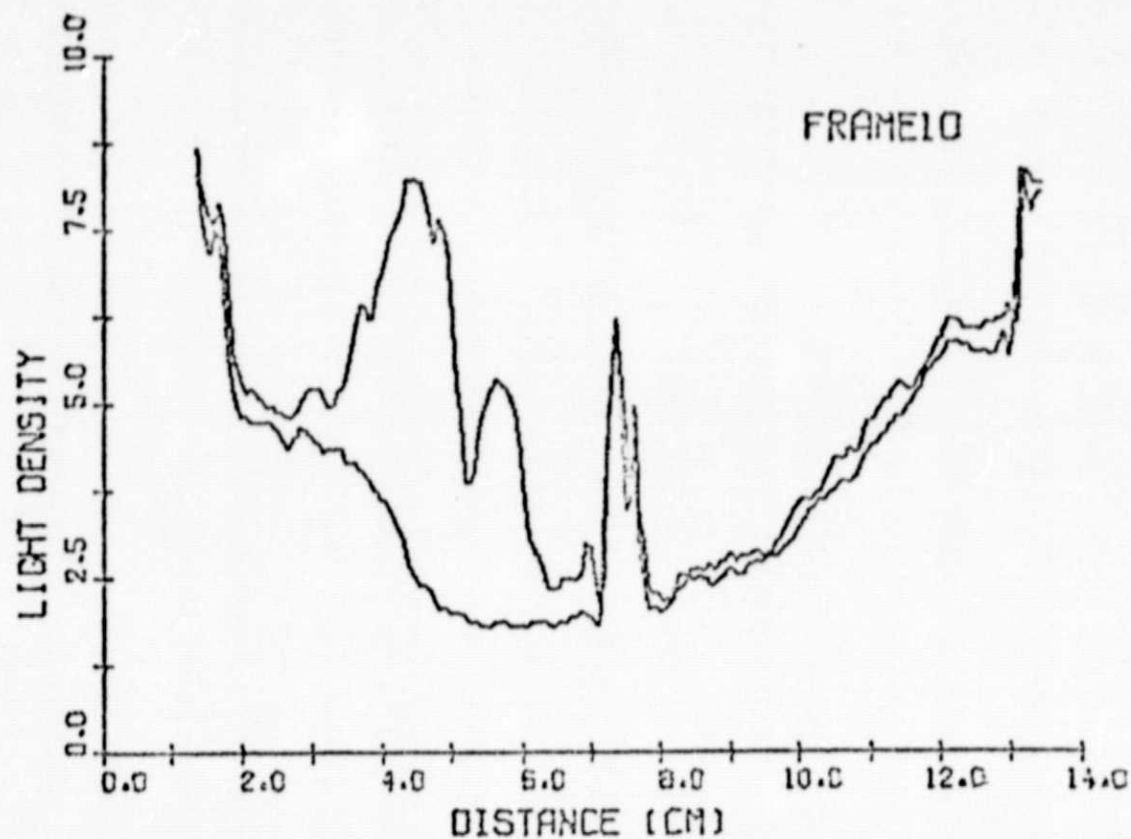


Figure 10. Micro-densitometer scan and computed displacement.  
 A. Raw data micro-densitometer scan for frames 1 and 10.  
 B. Net micro-densitometer scan and computed displacement.



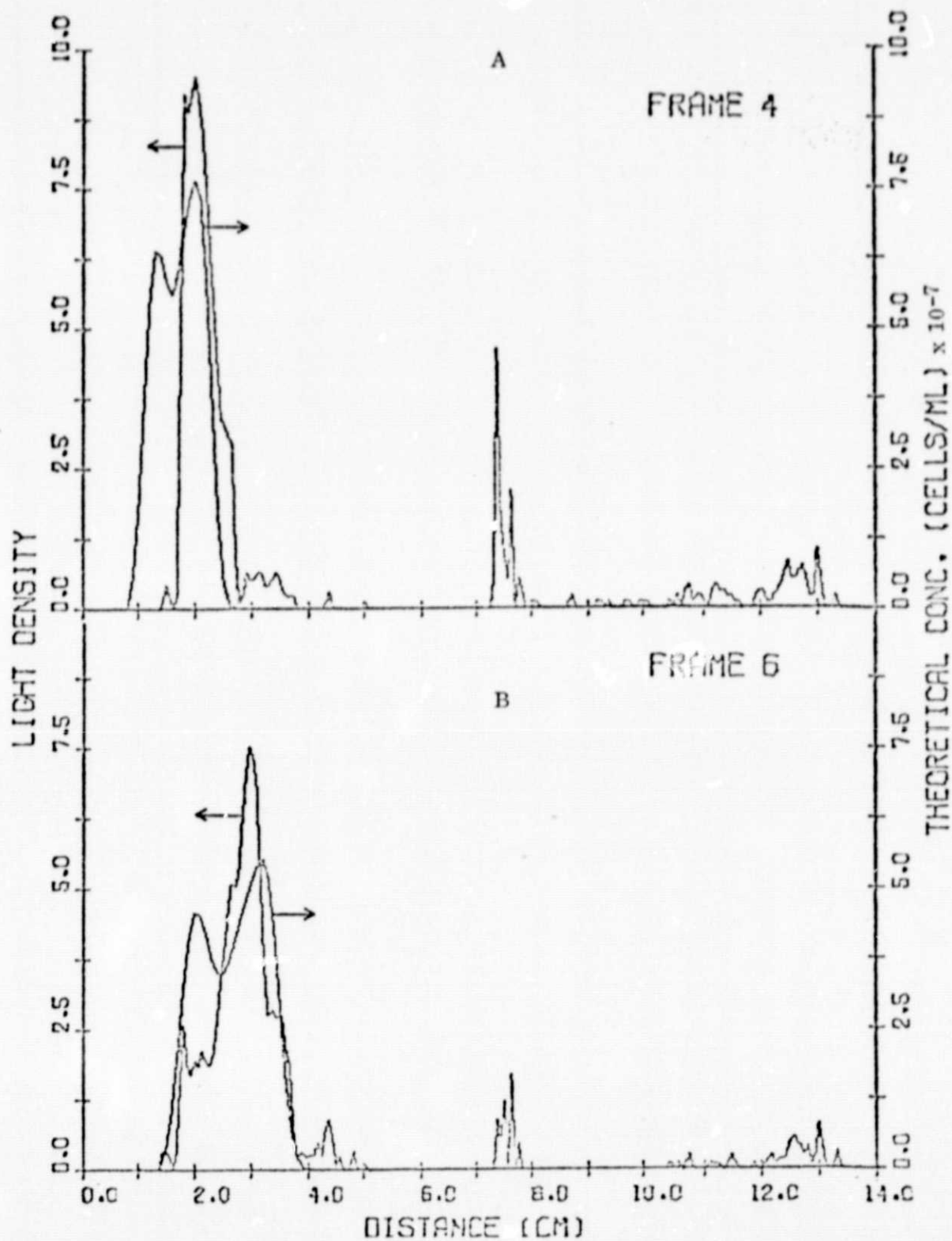


Figure 11. Micro-densitometer scan and computed displacement.

A. Frame 4, 12 minutes separation;

B. Frame 6, 18 minutes separation.

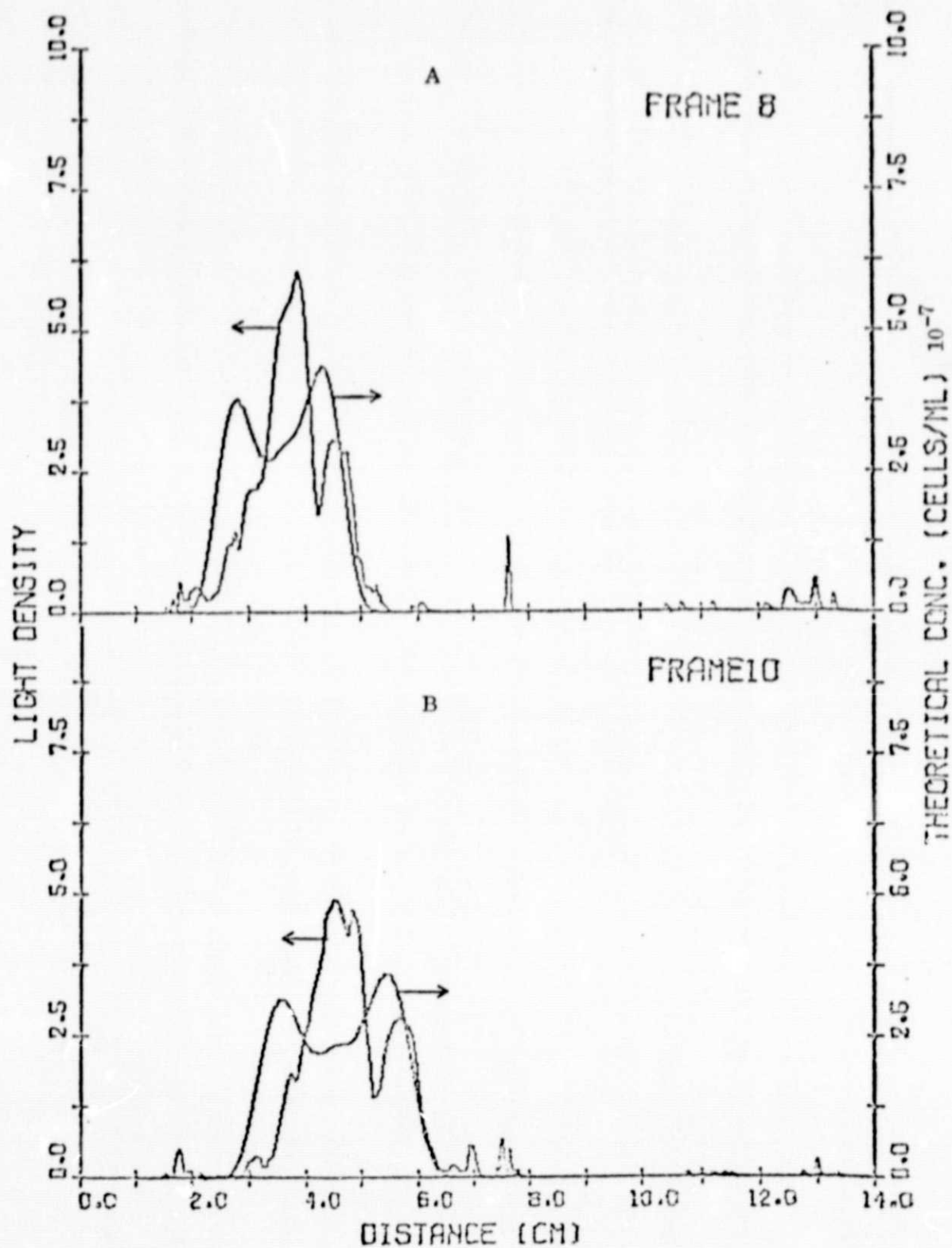


Figure 12. Micro-densitometer scan and computed displacement.  
 A. Frame 8, 24 minutes separation;  
 B. Frame 10, 30 minutes separation.

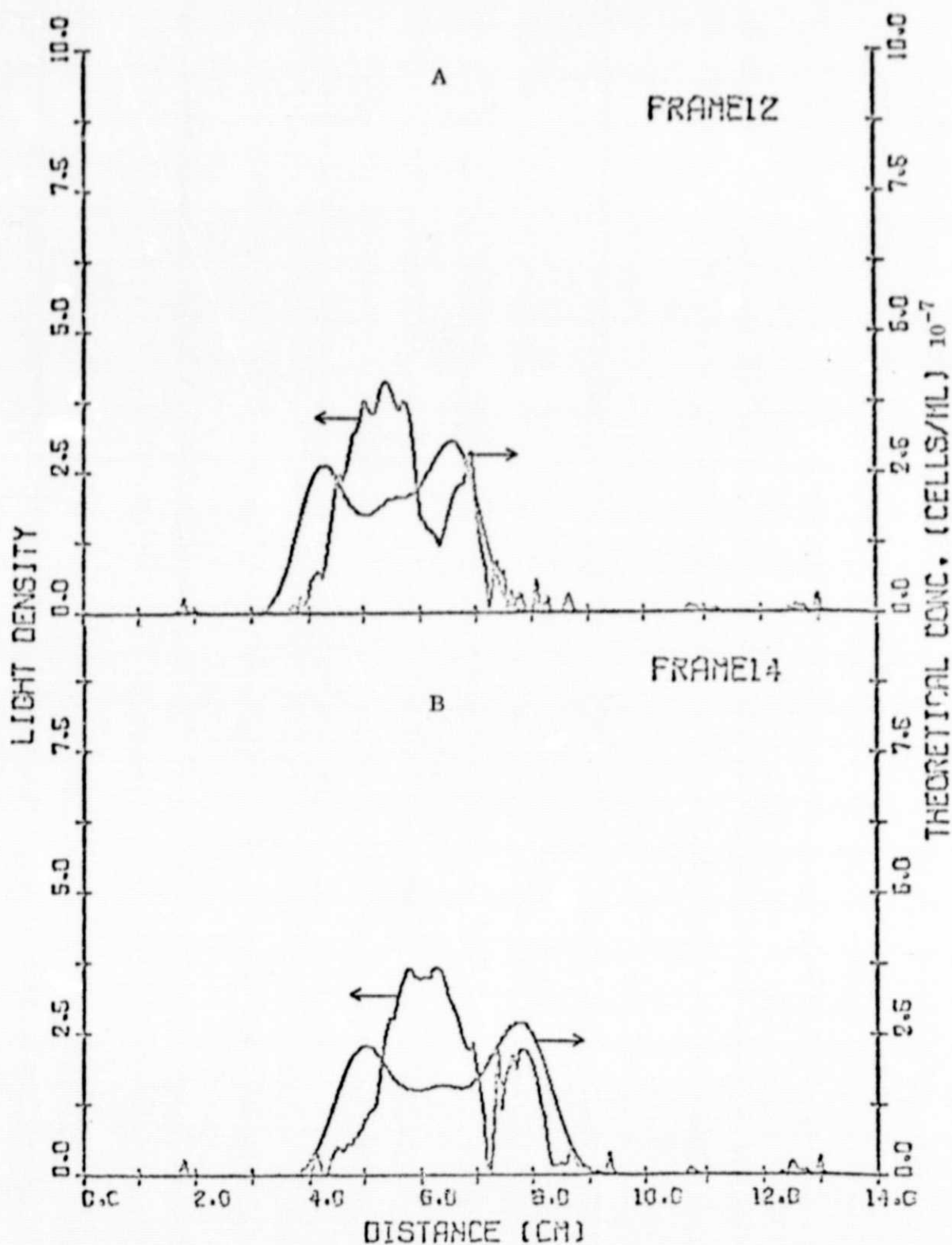
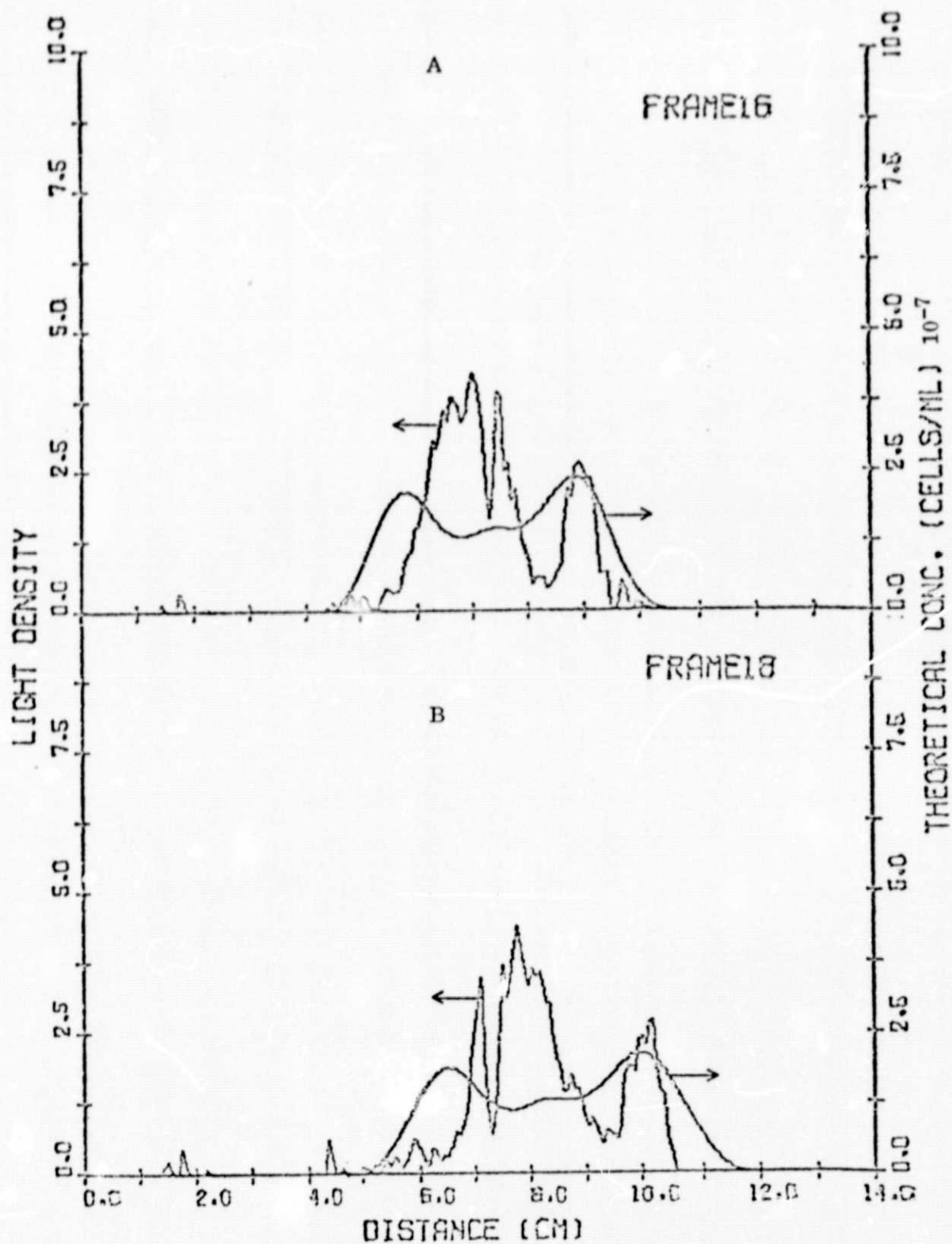


Figure 13. Micro-densitometer scan and computed displacement,  
 A. Frame 12, 36 minutes separation;  
 B. Frame 14, 42 minutes separation.





Frame 14. Micro-densitometer scan and computed displacement.  
 A. Frame 16, 48 minutes separation;  
 B. Frame 18, 52 minutes separation.

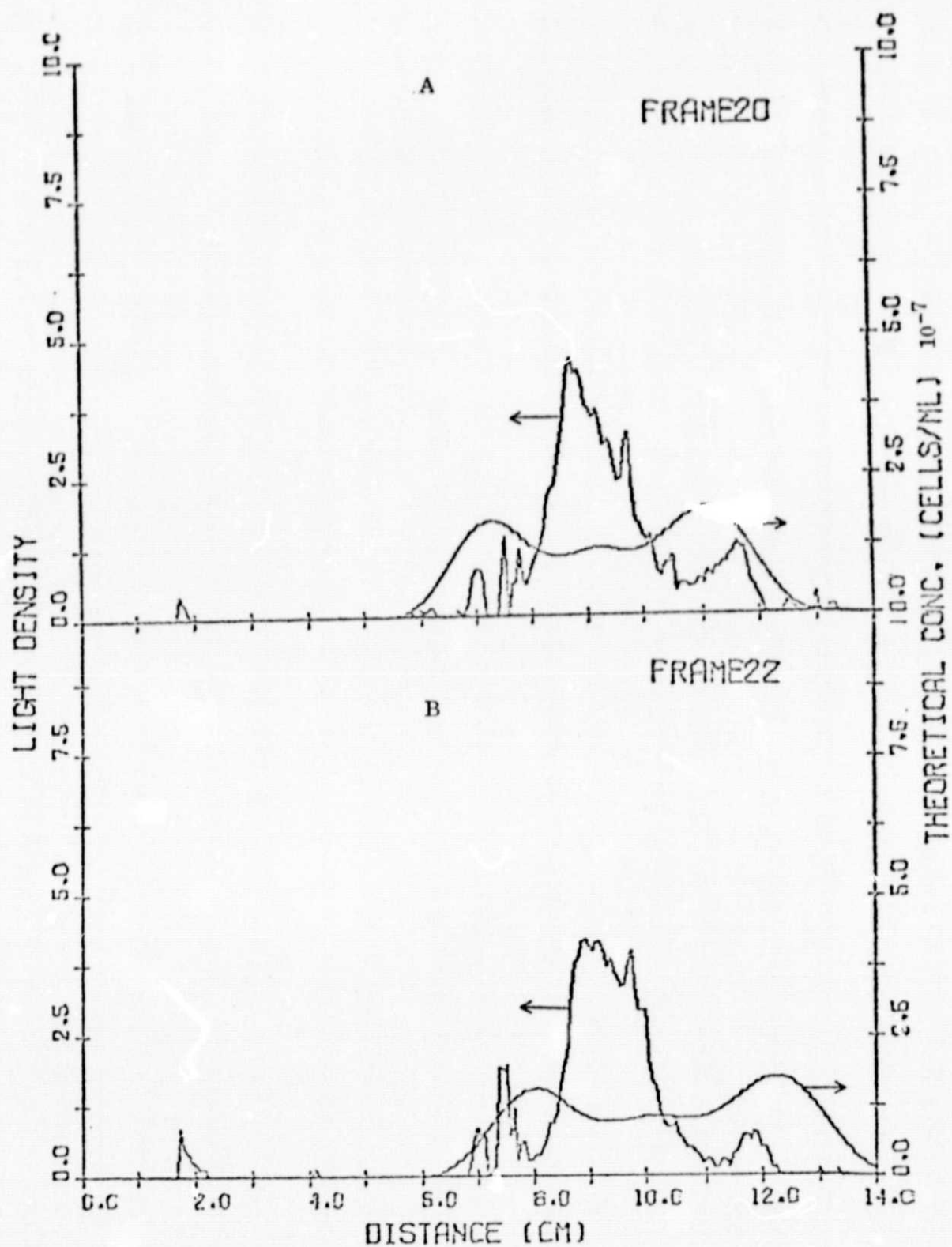


Figure 15. Micro-densitometer scan and computed displacement.  
 A. Frame 20, 60 minutes separation;  
 B. Frame 22, 66 minutes separation.

including photographic quality, the complex function between light density and cell concentration and type, and last of all the possibility of clumping by the cells. Although the specific effect of these considerations cannot be determined, the agreement between the micro-densitometer results and the theoretical predictions seems quite reasonable and would support both the theoretical model and the assigned experimental parameters.

### Conclusions

The electrophoretic separation of a mixture of three species of fixed red blood cells in space was successful in that fractionation according to mobility did occur and was found in the sliced samples although technical problems occurred in the operation of column 1 which was the subject of this analysis. Photographic evidence indicates that the low electroosmotic methylcellulose coating was successful in reducing the electroosmosis to a near zero value. Also the flight film shows that the bands migrated down the column as theory would predict, producing two bands of high cell concentration separated and surrounded by regions of lower cell concentration. However, most likely some clumping of the cells occurred to cause the trailing band to be larger than expected from theory.

The theoretical computer model gave good agreement with the experimental results, and was useful in defining the effect of the various experimental parameters. ~~The best resolution can be obtained by reducing  $U_{os}$~~  to near zero with as small a temperature gradient between channel center and wall as possible. The effect of  $U_{os}$  can be minimized by reducing the ratio of the sample plug radius to the channel radius but at the expense of sample volume. This can be compensated with little loss in resolution by increasing the sample plug thickness as long as this is negligible in relation to the total separation distance.

Overall, the experiment was a success in demonstrating a static electrophoresis separation under microgravity conditions with a resolution not possible on earth.

## References

1. McKannan, E. C., Krupnick, A. C., Griffin, R. N., and McCreight, L. R., "Electrophoresis Separation in Space - Apollo 14", NASA Technical Memorandum. TMX-64611 (1971).
2. Snyder, R.S., Bier, M., Griffin, R.N., Johnson, A.J., Leidheiser, H., Micale, F.J., Vanderhoff, J.W., Ross, S., van Oss, C.J., Separation and Purification Methods, 2 (2), 259-282 (1973).
3. Micale, F.J., Vanderhoff, J.W., "Electrophoresis Analysis for Apollo 16", Progress Report, Contract NAS8-28654 (1972).
4. Krumrine, P.H., "Coatings for Reduction of Electroosmosis and Factors Affecting Electrophoretic Separation Resolution", M.S. Thesis, October, 1976.
5. Vanderhoff, J.W., Micale, F.J., Krumrine, P.H., Separation and Purification Methods, 6 (1), 61-87 (1977).
6. Knox, R.J., "Electrophoretic Characterization of Aldehyde-Fixed Red Blood Cells, Kidney Cells, Lymphocytes and Chamber Coatings", Report No. NASA CR-2755, October, 1976.
7. Vanderhoff, J.W., Micale, F.J., "Final Report - Electrophoresis Experiment for Space", Contract No. NAS8-28654, April, 1976.

## APPENDIX



```

3      PROGRAM PHORESE (INPUT,OUTPUT,PLOT,TAPE99=PLOT)
3      DIMENSION W(25),Z(25)
3      DIMENSION FM1(192),FM2(192),PEAK(192),D(192)
3      COMMON/DRAW/ SHAPE(3,45),R(45),IMP
3      DIMENSION DIS(45)
3      COMMON//S1(10),S2(10),NA,NB,RATIO1,RATIO2,DIELECN,REVISM
3      COMMON/VAR/XLU,YLU,RU,RA,THETA,IPRINT
3      COMMON/SET/T1,T2,ALPHA,UOS,E
3      COMMON/SUB/UMEAN(3),UVARL(3),UVARR(3),AREA(3),AB(3),IDIST(3)
3      COMMON/TAB/QUEST(3,20),IORDER(3),JC(3)
3      COMMON/PT/ US(165),VS(165),VSA(3,165)
3      DATA WORD1,WORD2,WORD3/9H GAUSSIAN,9H TRIANGLE,9H PARABOLIC/
3      DATA WORD4,WORD5/9H SQUAPE,9H RANDOM/
1      READ 100,JA,NA
26      READ 101,(W(I),I=1,JA)
41      READ 101,(Z(I),I=1,JA)
43      NA1=NA+1
47      CALL LINEGEN(S1,NA,NA1,JA,W,Z)
57      READ 100,JB,NB
72      READ 101,(W(I),I=1,JB)
105      READ 101,(Z(I),I=1,JB)
107      NB1=NB+1
113      CALL LINEGEN(S2,NB,NB1,JB,W,Z)
133      READ 102,XLU,YLU,RU,RA,THETA,IPRINT
147      READ 103,UOS,T1,T2,E
155      READ 104,LOVE
161      PRINT 120
165      PRINT 110
171      PRINT 108
173      DO 1 I=1,LOVE
173      READ 105,UMEAN(I),UVARL(I),UVARR(I),AB(I),AREA(I),IDIST(I)
212      UEMAX=UMEAN(I)*UVARR(I)
215      UE=UMEAN(I)-UVARL(I)
217      IF(IDIST(I).EQ.1) WORD=WORD1
222      IF(IDIST(I).EQ.2) WORD=WORD2
226      IF(IDIST(I).EQ.3) WORD=WORD3
232      IF(IDIST(I).EQ.4) WORD=WORD4
236      IORDER(I)=0
240      IF(IDIST(I).NE.5) GO TO 4
242      WORD=WORD5
243      READ 106,JC(I)
251      K=JC(I)
253      READ 107,(W(J),J=1,K)
266      READ 107,(Z(J),J=1,K)
301      DO 5 J=1,K
303      5 QUEST(I,J)=Z(J)
312      CALL SEAPCH(W,Z,K,IC)
315      IORDER(I)=IC
317      4 CONTINUE
317      PRINT 109,I,UEMAX,UE,UMEAN(I),AREA(I),WORD,IORDER(I)
341      1 CONTINUE
344      PRINT 110
347      PRINT 112,E
355      PRINT 114,UOS
363      PRINT 110
367      PRINT 116,THETA
375      PRINT 117,RA
403      PRINT 110
407      PRINT 115,T1 2
417      PRINT 120
423      DO 2 N=1,161
425      US(N)=-1.0+(N-1)/10.0
432      IF(US(N).LT.0.0) US(N)=0.0
435      IF(US(N).GT.14.0) US(N)=14.0
442      JC 25 M=1,LOVE
444      VSA(M,N)=0.0
451      VS(N)=0.0
455      DIELEC1=ZAM(S1,NA,T1)
460      DIELEC2=ZAM(S1,NA,T2)
463      DIELECN=ZAM(S1,NA,299.0)
466      REVISM1=ZAM(S2,NB,T1)
471      REVISM2=ZAM(S2,NB,T2)
476      REVISM=ZAM(S2,NB,299.0)
477      RATIO1=(DIELEC1*REVISM)/(DIELECN*REVISM1)
492      RATIO2=(DIELEC2*REVISM)/(DIELECN*REVISM2)
505      READ 111,NUM,NFRAME,NSLIDE

```

ORIGINAL PAGE IS  
OF POOR QUALITY

```

517 ALPHA=0.0
520 TIMET=3.0*60.0/10000.0*NFRAME
523 CALL ACTUAL (TIMET,LOVE)
525 CALL CONCENT (TIMET,LOVE)
527 PRINT 110
533 READ 113, (FM2(I), I=1, NUM)
546 READ 113, (FM1(I), I=1, NUM)
561 SUMA=0.0
562 DO 7 I=1, NUM
564 PEAK(I)=FM2(I)-NSLIDE-FM1(I)
570 O(I)=(13.0+I*0.6394736842)*0.1
575 IF (PEAK(I).LT.0.0) PEAK(I)=0.0
600 SUMA=SUMA+PEAK(I)
603 7 CONTINUE
605 SUM=0.0
606 DO 3 N=1, 161
607 3 SUM=SUM+VS(N)
613 FACTAR=1.485566E7/SUM
615 DO 6 N=1, 161
616 DO 24 M=1, LOVE
617 24 VSA(M,N)=VSA(M,N)*FACTAR/1.7945E-2
626 6 VS(N)=VS(N)*FACTAR/1.7945E-2
633 UPGRADE=0.1/0.06394736842
634 FACTER=828.2/SUMA
636 DO 8 N=1, NUM
640 8 PEAK(N)=PEAK(N)*UPGRADE*FACTER
646 CALL NAMPLT
647 CALL FACTOR(0.9)
651 IF (IPRINT.NE.1) GO TO 22
653 CALL FACTOR(1.2)
655 22 CONTINUE
655 CALL PLOT(0.0, -0.5, -3)
660 FM1(NUM+1)=0.0
662 FM1(NUM+2)=25.0
664 FM2(NUM+1)=0.0
665 FM2(NUM+2)=25.0
667 D(NUM+1)=0.0
670 D(NUM+2)=2.54
672 PEAK(NUM+1)=0.0
673 PEAK(NUM+2)=25.0
675 US(162)=0.0
676 US(163)=2.54
677 VS(162)=0.0
700 VS(163)=2.5E7
701 R(IMP+1)=-1.0
703 R(IMP+2)=2.54
705 DIS(IMP+1)=0.0
707 DIS(IMP+2)=2.54
710 IF (IPRINT.NE.5) GO TO 30
712 CALL FACTOR(1.1)
713 CALL AXIS1(1.5, 1.5, 33H
10, 0.0, 2.5E7, 20.0)
724 CALL AXIS1(1.5, 1.5, 13H
735 CALL SYMROL(2.8, 0.75, 0.125, 26H
741 CALL PLOT(1.5, 1.5, -3)
744 CALL LINE(US, VS, 161, 1, 0, 0)
750 DO 26 I=1, LOVE
752 DO 27 J=1, 161
753 27 VS(J)=VSA(I, J)
762 CALL PLOT(0.0, 0.0, 3)
764 CALL LINE(US, VS, 161, 1, 0, 0)
770 26 CONTINUE
773 CALL PLOT(0.0, 2.5, -3)
775 DO 28 I=1, LOVE
777 DO 29 J=1, IMP
1000 29 DIS(J)=SHAPE(I, J)
1007 CALL LINE(DIS, R, IMP, 1, 0, 0)
1013 CALL PLOT(0.0, 0.0, 3)
1016 28 CONTINUE
1021 CALL PLOT(-1.5, -4.0, -3)
1023 30 CONTINUE
1023 IF (IPRINT.EQ.5) GO TO 19
1025 IF (IPRINT.EQ.3) GO TO 18
1027 CALL AXIS1(1.5, 1.5, 13H
1037 CALL AXIS1(1.5, 1.5, 13H
1050 CALL AXIS1(7.012, 1.5, 33H

```

ORIGINAL PAGE IS  
OF POOR QUALITY

THEORETICAL CONC. (CELLS/ML), 33, 4.0, 90.

10, 0.0, 2.5E7, 20.0) DISTANCE (CM), -13.5, 512, 0.0, 0.0, 2.54, 25.4)  
COMPUTED CELL DISPLACEMENT, 0.0, 26)

THEORETICAL CONC. (CELLS/ML), -33, 4.0,

190.2, 0.0, 2.5E7, 20.0)

1061

1065

1071

1075

1100

1104

1107

1113

1116

1120

1123

1125

1128

1135

1141

1144

1147

1151

1151

1153

1164

1175

1201

1205

1207

1211

1215

1220

1224

1227

1233

1236

1236

1241

1242

1253

1264

1266

1267

1270

1271

1273

1274

1275

1302

1306

1310

1312

1313

1315

1321

1326

1330

1332

1336

1337

1341

1342

1343

1346

1352

1354

1355

1364

1367

1373

1376

1378

1401

1402

1402

1402

1402

1402

```

CALL SYMBOL(1.65,0.6,0.125,49MICRO-DENSITOMETER SCAN AND COMPUTE
1 DISPLACEMENT,0.0,49)
CALL SYMBOL(5.5,5.0,0.15,5HFRAME,0.0,5)
CALL NUMBER(6.125,5.0,0.15,NFRAME,0.0,2HI2)
CALL PLOT(1.5,1.5,-3)
CALL LINE(0,PEAK,NUM,1,0,0)
CALL PLOT(0.0,0.0,3)
CALL LINE(US,VS,161,1,0,0)
CALL PLOT(-1.5,-1.5,-3)
IF(IPRINT.NE.1) GO TO 21
CALL PLOT(1.5,4.0,-3)
DO 20 I=1,LOVE
DO 17 J=1,IMP
17 DIS(J)=SHAPE(I,J)
CALL LINE(DIS,0,IMP,1,0,0)
CALL PLOT(0.0,0.0,3)
2) CONTINUE
CALL PLOT(-1.5,-4.0,-3)
21 CONTINUE
IF(IPRINT.EQ.1) GO TO 18
CALL AXIS1(1.5,6.5,13HLIGHT DENSITY,13,4.0,90.0,0.0,25.0,20.0)
CALL AXIS1(1.5,6.5,13HDISTANCE (CM),-13,5.512,0.0,0.0,2.54,25.4)
CALL SYMBOL(5.5,10.0,0.15,5HFRAME,0.0,5)
CALL NUMBER(6.125,10.0,0.15,NFRAME,0.0,2HI2)
DO 9 N=1,NUM
FM1(N)=FM1(N)/1.5
9 FM2(N)=FM2(N)/1.5
CALL PLOT(1.5,6.5,-3)
CALL LINE(0,FM1,NUM,1,0,0)
CALL PLOT(0.0,0.0,3)
CALL LINE(0,FM2,NUM,1,0,0)
CALL PLOT(8.0,-6.5,-3)
13 CONTINUE
IF(IPRINT.LT.3) GO TO 19
CALL FACTOR(1.0)
CALL AXIS1(1.5,3.0,14HRELATIVE CONC.,14,5.0,90.0,0.0,20.0,20.0)
CALL AXIS1(1.5,3.0,24HELECTROPHORETIC MOBILITY,-24,7.880,0.0,0.0,0.0)
1.635,29.4)
T1=298.0
T2=298.0
UOS=0.0
THETA=0.0001
TIMET=0.264
DO 12 N=1,161
DO 23 K=1,LOVE
23 VSA(K,N)=0.0
12 VS(N)=0.0
CALL ACTUAL (TIMET,LOVE)
CALL CONCENT (TIMET,LOVE)
XMAX=0.0
DO 10 N=1,161
IF(VS(N).GT.XMAX) XMAX=VS(N)
10 US(N)=US(N)/(E*TIMET)
FACTOR=XMAX/100.0
DO 11 N=1,161
VS(N)=VS(N)/FACTOR
US(162)=0.0
US(163)=0.635
VS(162)=0.0
VS(163)=20.0
CALL PLOT(1.5,3.0,-3)
CALL LINE(US,VS,161,1,0,0)
DO 13 L=1,LOVE
DO 16 N=1,161
16 VS(N)=VSA(L,N)/FACTOR
CALL PLOT(0.0,0.0,3)
CALL LINE(US,VS,161,1,0,0)
13 CONTINUE
19 CONTINUE
CALL PLOT(10.0,-1.5,-3)
CALL ENDPLT
101 FORMAT(2I2)
101 FORMAT(8S10.3)
102 FORMAT(5(F8.3),I2)
103 FORMAT(4(F8.3))
104 FORMAT(3(I5))
105 FORMAT(5(F8.3),2X,I1)

```

ORIGINAL PAGE IS  
OF POOR QUALITY



```

1402 135 FORMAT(I2)
1402 137 FORMAT(8E10.0)
1402 138 FORMAT(19X,4HLEAD,3X,5HTRAIL,4X,4HPEAK,4X,4HAREA,6X,5HSHAPE,3X,5H
1402 139 /)
1402 139 FORMAT(1X,*PARTICLE NO.*,I2,4(F8.3),2X,A9,6X,I2)
1402 140 FORMAT(7/)
1402 141 FORMAT(I3,2(IX,I2))
1402 142 FORMAT(5X,21HPOTENTIAL GRADIENT = ,F5.1,*VOLTS/CM*)
1402 143 FORMAT(2CE4.3)
1402 144 FORMAT(5X,*UOS = ,F6.2,*MICRON CM/VOLT SEC*)
1402 145 FORMAT(5X,*WALL TEMPERATURE = ,F10.4,*DEGREES K*,/,5X,*CENTER TEMP
1402 146 ERATURE = ,F10.4,*DEGREES K*)
1402 147 FORMAT(5X,*THETA = ,F5.2,*CM*)
1402 148 FORMAT(5X,*SAMPLE RADIUS = ,F4.3)
1402 149 FORMAT(1X,/,*XXXXXXXXXXXXXXXXXXXXXXXXXXXXXXXXXXXXXXXXXXXXXXXXXXXX
1402 150 XXXXXXXXXXXXXXXXXXXX*,/)
1402 151 CALL EXIT
1402 152 END

```

```

5 SUBROUTINE ACTUAL (TIME,LOVE)
5 DIMENSION DF(3,21),DP(3,21)
5 COMMON/DPAW/ SHAPE(3,45),R(45),IMP
5 COMMON//S1(10),S2(10),NA,NB,RATIO1,RATIO2,DIELECN,REVISN
5 COMMON/VAR/XLU,YLU,PU,RA,THEIA,IPRINT
5 COMMON/SET/T1,T2,ALPHA,UOS,E
5 COMMON/ZVAL/ Z,KIMP
5 COMMON/SUB/UMEAN(3),UVARL(3),UVAPR(3),AREA(3),AB(3),IOIST(3)
5 FIN=1.0E10
5 CEN=0.0
5 RUT=RA
5 KIMP=0
5 IMAX=2.0*RUT/0.1+1.5
5 RUM=CEN
5 DO 4 K=1,2
5 IF(K.EQ.2) RUM=PA
5 T3=T2-(T2-T1)*ABS(RUM)**2
5 DIELEC3=ZAM(S1,NA,T3)
5 REVIS3=ZAM(S2,NB,T3)
5 RATIO3=(DIELEC3*REVISN)/(DIELECN*REVIS3)
5 POSIT=2.0*PU**2-1.0
5 DTFIN=((UMEAN(1)-UVAPL(1))*RATIO3+UOS*POSIT*RATIO1)*E*TIME-THEIA
5 IF(DTFIN.LT.FIN) FIN=DTFIN
5 4 CONTINUE
5 SCALE=YLU+FIN-1.0
5 ISCALE=SCALE
5 7=ISCALE
5 DO 32 I=1,IMAX
5 IF(RUT.GT.RA+0.01) GO TO 29
5 IF(RUT.LT.-RA-0.01) GO TO 29
5 T3=T2-(T2-T1)*ABS(RUT)**2
5 DIELEC3=ZAM(S1,NA,T3)
5 REVIS3=ZAM(S2,NB,T3)
5 RATIO3=(DIELEC3*REVISN)/(DIELECN*REVIS3)
5 POSIT=2.0*PU**2-1.0
5 IM=2*IMAX-I+1
5 DO 28 M=1,LOVE
5 DF(M,I)=((UMEAN(M)+UVAPR(M))*RATIO3+UOS*POSIT*RATIO1)*E*TIME+YLU-
5 DP(M,I)=((UMEAN(M)-UVARL(M))*RATIO3+UOS*POSIT*RATIO1)*E*TIME+YLU-
5 1 THEIA
5 SHAPE(M,I)=DF(M,I)
5 R(I)=RUT
5 SHAPE(M,IM)=DP(M,I)
5 R(IM)=RUT
5 K1=(DF(M,I)-Z)*10.0+5.0
5 IF(K1.GT.KIMP) KIMP=K1
5 23 CONTINUE
5 29 CONTINUE
5 RUT=RUT-0.1
5 32 CONTINUE
5 IMP=2*IMAX+1
5 DO 5 M=1,LOVE
5 SHAPE(M,IMP)=DF(M,1)
5 R(IMP)=P(1)
5 RETURN
5 END

```

ORIGINAL PAGE IS  
OF POOR QUALITY

```

SUBROUTINE CONCENT(TIME, LOVE)
DIMENSION P(20), Q(20), UGH(10), G(3), F(3)
DIMENSION Y(250), SUM(4, 250)
COMMON//S1(10), S2(10), NA, NB, RATIO1, RATIO2, DIELECN, REVISN
COMMON/VAR/XLU, YLU, RU, RA, THETA, IPRINT
COMMON/SET/T1, T2, ALPHA, UCS, E
COMMON/ZVAL/ Z, KIMP
COMMON/SUB/UMEAN(3), UVARL(3), UVARR(3), AREA(3), AB(3), IDIST(3)
COMMON/TAB/QUEST(3, 20), ICRDER(3), JC(3)
COMMON/PT/ US(165), VS(165), VSA(3, 165)
DATA PI/3.141592654/
GEN=0.0
IMAX=2.0*RU/0.05+1.1
IF(KIMP.GT.131) KIMP=131
DO 19 M=1, LOVE
DO 1 J=1, KIMP
1 SUM(M, J)=0.0
RUT=RU
DO 17 I=1, IMAX
IF(RUT.GT.CEN+RA+0.01) GO TO 16
IF(RUT.LT.CEN-RA-0.01) GO TO 16
XMULT=2.0*PI*ABS(RUT)
T3=T2-(T2-T1)*ABS(RUT)**2
DIELEC3=ZAM(S1, NA, T3)
REVIS3=ZAM(S2, NB, T3)
RATIO3=(DIELEC3*REVISN)/(DIELECN*REVIS3)
POSIT=2.0*RUT**2-1.0
DT=(UMEAN(M)*RATIO3+UCS*POSIT*RATIO1)*E*TIME
DL=UVARL(M)*E*RATIO3*TIME+THETA/2.0
DR=UVARR(M)*E*RATIO3*TIME+THETA/2.0
ATHE=DT*10.0
THE=(DT-DL)*10.0
LTHE=LTHE
XTHE=LTHE
DTHE=1.0-(THE-XTHE)
YUM=DL*10.0
WUM=DR*10.0
NYUM=YUM-DTHE
DIST=ABS(DL+DR)*10.0
LDIST=DIST
IF(LDIST.LT.1) LDIST=1
AC=AB(M)
MCOUNT=0
KTEL=IDIST(M)
GO TO (40, 46, 48, 50, 7) KTEL
7 NAC=ICRDER(M)+1
NAC1=NAC+1
THE=DT*10.0
LTHE=LTHE
XTHE=LTHE
DTHE=1.0-(THE-XTHE)
JOY=JC(M)
PLUS=DIST/(JOY-1)
DO 6 K=1, JOY
P(K)=THE+(K-1)*PLUS
Q(K)=QUEST(M, K)
6 CONTINUE
CALL LINEGEN(UGH, NAC, NAC1, JOY, P, Q)
DO 8 K=1, LDIST
Y(K)=0.0
XNUM=THE+DTHE+K-1
Y(K)=ZAM(UGH, NAC, XNUM)
8 IF(Y(K).LT.0.0) Y(K)=0.0
GO TO 52
40 JOG1=1.0/YUM
JOG2=1.0/WUM
SAME=0.0
DO 41 K=1, 40
XNUM=THE+DTHE+(1-K)
YK=AC*EXP(-(JOG1**2)*(XNUM-ATHE)**2)
IF(YK.LT.AC*0.01) GO TO 42
MCOUNT=MCOUNT+1
41 CONTINUE
42 DO 44 K=1, 70
XNUM=XNUM+1
Y(K)=AC*EXP(-(JOG1**2)*(XNUM-ATHE)**2)

```

ORIGINAL PAGE IS  
OF POOR QUALITY

```

306 IF(Y(K).LT.SAME) GO TO 43
312 SAME=Y(K)
313 GO TO 44
313 43 Y(K)=AC*EXP(-(DOG2**2)*(XNUM-ATHE)**2)
323 IF(Y(K).LT.0.01*AC) GO TO 45
330 44 CONTINUE
332 45 LDIST=K
334 GO TO 52
334 46 SLOPER=AC/WUM
336 SLOPEL=AC/YUM
340 RL=AC-SLOPEL*ATHE
342 BR=AC+SLOPER*ATHE
344 DO 47 K=1,LDIST
346 XNUM=THE+OTHE+(K-1)
353 Y(K)=SLOPEL*XNUM+BL
356 IF(K.GT.NYUM) Y(K)=-SLOPER*XNUM+BR
364 IF(Y(K).GT.AC) Y(K)=AC
371 47 IF(Y(K).LT.0.0) Y(K)=0.0
377 GO TO 52
377 48 Q(1)=0.0
400 Q(2)=AB(M)
402 Q(3)=0.0
403 P(2)=ATHE
404 P(1)=ATHE-YUM
406 P(3)=ATHE+YUM
407 CALL LINEGEN(G,3,4,3,P,0)
413 P(1)=ATHE-WUM
415 P(3)=ATHE+WUM
417 CALL LINEGEN(F,3,4,3,P,0)
423 DO 49 K=1,LDIST
426 XNUM=THE+OTHE+(K-1)
433 Y(K)=ZAM(G,3,XNUM)
440 IF(K.GT.NYUM) Y(K)=ZAM(F,3,XNUM)
451 49 IF(Y(K).LT.0.0) Y(K)=0.0
457 GO TO 52
457 50 DO 51 K=1,LDIST
461 51 Y(K)=AC
465 52 CONTINUE
465 TOTAL=0.0
466 DO 10 K=1,LDIST
470 10 TOTAL=TOTAL+Y(K)
474 ADJUST=APEA(M)/TOTAL
477 DO 11 K=1,LDIST
500 11 Y(K)=Y(K)*ADJUST*XMULT
506 LIM1=1
507 LIM2=0
510 NWIDTH=THETA*10.0
512 IF(NWIDTH.LT.1) NWIDTH=1
515 NO=LDIST+NWIDTH-1
517 J=ABS(7-UT+OL+THETA-YLU)*10.0-MC CUNT+2
532 DO 14 L=1,NO
533 IF(L.GT.NWIDTH) LIM1=LIM1+1
537 LIM2=LIM2+1
541 IF(LIM2.GT.LDIST) LIM2=LDIST
544 DO 13 K=LIM1,LIM2
546 13 SUM(M,J)=SUM(M,J)+Y(K)
555 J=J+1
557 14 CONTINUE
561 15 CONTINUE
561 RUT=RUT-0.05
563 17 CONTINUE
566 TOSUM=0.0
567 DO 9 J=1,KIMP
570 9 TOSUM=TOSUM+SUM(M,J)
575 ADJ=APEA(M)/TOSUM
601 DO 12 J=1,KIMP
602 12 SUM(M,J)=SUM(M,J)*ADJ
610 19 CONTINUE
613 LOVE1=LOVE+1
614 DO 20 K=1,KIMP
616 SUM(LOVE1,K)=0.0
621 DO 20 I=1,LOVE
622 20 SUM(LOVE1,K)=SUM(LOVE1,K)+SUM(I,K)
635 IF(ALPHA.EQ.1.0) GO TO 25
637 YK=0.0
640 DO 21 K=1,KIMP
642 XK=SUM(LOVE1,K)

```

ORIGINAL PAGE IS  
OF POOR QUALITY

```

645 IF(XK.GT.YK) YK=XK
650 21 CONTINUE
653 FACTOR=YK/100.0
655 25 CONTINUE
658 NOX=(Z+1.0)*10.0
661 DO 35 M=1,KIMP
662 YCRE=NOX*M
664 IF(MORE.GT.161) MORE=161
667 DO 36 K=1,LOVE
671 36 VSA(K,MORE)=VSA(K,YCRE)+SUM(K,M)/FACTOR
703 VS(MORE)=VS(MORE)+SUM(LOVE1,M)/FACTOR
710 35 CONTINUE
712 RETURN
713 END

```

```

11 SUBROUTINE LINEGEN(S,NA,NA1,JA,X,Y)
11 DIMENSION X(JA),Y(JA),S(NA)
11 COMMON/NEED/ A(10,11)
11 DO 3 I=1,NA
12 DO 2 J=1,NA
13 BNUM=0.0
14 DO 1 K=1,JA
16 BNUM=BNUM+X(K)**(I+J-2)
25 1 CONTINUE
27 A(I,J)=BNUM
33 2 CONTINUE
35 3 CONTINUE
37 DO 5 L=1,NA
40 CNUM=0.0
41 DO 4 K=1,JA
43 CNUM=CNUM+Y(K)*X(K)**(L-1)
54 4 CONTINUE
56 A(L,NA1)=CNUM
61 5 CONTINUE
63 CALL GAUSS(S,NA,NA1)
64 RETURN
65 END

```

```

6 SUBROUTINE GAUSS (X,N,NP1)
6 DIMENSION X(N)
6 COMMON/NEED/ A(10,11)
6 NM1=N-1
10 DO 4 K=1,NM1
11 KP1=K+1
13 L=K
14 DO 1 I=KP1,N
16 1 IF(ABS(A(I,K)).GT.ABS(A(L,K))) L=I
33 IF(L.EQ.K) GO TO 3
35 DO 2 J=K,NP1
36 TEMP=A(K,J)
41 A(K,J)=A(L,J)
46 2 A(L,J)=TEMP
53 3 DO 4 I=KP1,N
55 FACTOR=A(I,K)/A(K,K)
62 DO 4 J=KP1,NP1
64 A(I,J)=A(I,J)-FACTOR*A(K,J)
103 X(N)=A(N,NP1)/A(N,N)
111 I=NM1
112 5 KP1=I+1
114 SUM=0.0
116 DO 6 J=KP1,N
117 6 SUM=SUM+A(I,J)*X(J)
131 X(I)=(A(I,NP1)-SUM)/A(I,I)
140 I=I-1
141 IF(I.GE.1) GO TO 5
143 RETURN
145 END

```

ORIGINAL PAGE IS  
OF POOR QUALITY



```

7      SUBROUTINE SEARCH(X,Y,J,I0)
7      DIMENSION X(J),Y(J),S(10),XSUM(10)
10     RSUM=1.0E100
11     LOVE=6
13     DO 3 N=2,LOVE
13     NA=N
13     NA1=NA+1
15     NA1=NA-1
15     CALL LINEGEN(S,NA,NA1,J,X,Y)
23     SUM=0.0
24     DO 2 I=1,J
30     YC=0.0
31     XA=X(I)
33     YC=7*AM(S,NA,XA)
35     YE=Y(I)
42     YA=YB-YC
44     SUM=SUM+YA**2
46     2 CONTINUE
50     XSUM(NA)=SUM
52     IF(XSUM(NA).LT.PSUM) RSUM=XSUM(NA)
55     3 CONTINUE
60     DO 4 I=2,LOVE
61     4 IF(RSUM.EQ.XSUM(I)) GO TO 5
66     5 I0=I-1
70     RETURN
76     END

```

```

6      FUNCTION ZAM(S,N,T)
6      DIMENSION S(N)
7      YC=0.0
7      DO 1 J=1,N
10     1 YC=YC+S(J)*T**(J-1)
22     ZAM=YC
23     RETURN
23     END

```

ORIGINAL PAGE IS  
OF POOR QUALITY



FWA OF THE LOAD 111  
LWA+1 OF THE LOAD 27456

TRANSFER ADDRESS -- PHORESE 2227

## PROGRAM AND BLOCK ASSIGNMENTS.

| BLOCK   | ADDRESS | LENGTH | FILE       | DATE     | PROCSSR | VER | LEVEL | HAR      |
|---------|---------|--------|------------|----------|---------|-----|-------|----------|
| /DRAW/  | 111     | 265    |            |          |         |     |       |          |
| /VAR/   | 376     | 6      |            |          |         |     |       |          |
| /SET/   | 404     | 5      |            |          |         |     |       |          |
| /SUB/   | 411     | 22     |            |          |         |     |       |          |
| /TAB/   | 433     | 102    |            |          |         |     |       |          |
| /PT/    | 535     | 1471   |            |          |         |     |       |          |
| PHORESE | 2226    | 6607   | LGO        | 07/21/77 | RUN     | F   | EB    | 74 B 646 |
| /ZVAL/  | 11035   | 2      |            |          |         |     |       |          |
| ACTUAL  | 11037   | 467    | LGO        | 07/21/77 | RUN     | F   | EB    | 74 B 646 |
| CONCENT | 11526   | 3457   | LGO        | 07/21/77 | RUN     | F   | EB    | 74 B 646 |
| /NEED/  | 15205   | 156    |            |          |         |     |       |          |
| LINEGEN | 15363   | 77     | LGO        | 07/21/77 | RUN     | F   | EB    | 74 B 646 |
| GAUSS   | 15462   | 161    | LGO        | 07/21/77 | RUN     | F   | EB    | 74 B 646 |
| SEARCH  | 15643   | 134    | LGO        | 07/21/77 | RUN     | F   | EB    | 74 B 646 |
| ZAM     | 15777   | 31     | LGO        | 07/21/77 | RUN     | F   | EB    | 74 B 646 |
| ACCOER  | 16030   | 12     | SL-RUN2P3  | 03/14/75 | COMPASS | 3.  |       | 74224    |
| EXP     | 16042   | 57     | SL-RUN2P3  | 03/14/75 | COMPASS | 3.  |       | 74224    |
| SINGOS  | 16121   | 77     | SL-RUN2P3  | 03/14/75 | COMPASS | 3.  |       | 74224    |
| LINE    | 16220   | 304    | SL-RUN2P3  | 04/18/75 | RUN     | 2   | .3    | 75073    |
| NCHAZ   | 16524   | 43     | SL-RUN2P3  | 04/18/75 | COMPASS | 3.  |       | 74224    |
| AXIS1   | 16567   | 545    | SL-RUN2P3  | 05/27/75 | RUN     | 2   | .3    | 75073    |
| SYSTEM  | 17334   | 1115   | SL-RUN2P3  | 01/08/76 | COMPASS | 3.  |       | 2-406    |
| OUTPTS  | 20451   | 70     | SL-RUN2P3  | 01/08/76 | COMPASS | 3.  |       | 2-406    |
| PRATEX  | 20541   | 41     | SL-RUN2P3  | 01/08/76 | COMPASS | 3.  |       | 2-406    |
| GETBA   | 20602   | 17     | SL-RUN2P3  | 01/08/76 | COMPASS | 3.  |       | 2-406    |
| INPUTC  | 20621   | 121    | SL-RUN2P3  | 01/08/76 | COMPASS | 3.  |       | 2-406    |
| OUTPTC  | 20742   | 72     | SL-RUN2P3  | 01/08/76 | COMPASS | 3.  |       | 2-406    |
| SIDS    | 21034   | 1475   | SL-RUN2P3  | 01/08/76 | COMPASS | 3.  |       | 2-406    |
| R23RCVR | 22531   | 166    | SL-RUN2P3  | 07/02/76 | COMPASS | 3.  |       | 2-410    |
| PLOI    | 22717   | 2000   | SL-RUN2P3  | 03/31/77 | COMPASS | 3.  |       | 3-428    |
| KODER   | 24717   | 1300   | SL-RUN2P3  | 04/22/77 | COMPASS | 3.  |       | 3-439    |
| NUMBER  | 26217   | 62     | SL-RUN2P3  | 04/18/75 | RUN     | 2   | .3    | 75073    |
| WPAKER  | 26301   | 1064   | SL-RUN2P3  | 04/22/77 | COMPASS | 3.  |       | 3-439    |
| SYS.RM  | 27355   | 37     | SL-NUCLEUS | 07/02/76 | COMPASS | 3.  |       | 2-410    |
| //      | 27424   | 32     |            |          |         |     |       |          |

1.005 CP SECONDS

415008 CM STORAGE USED

ORIGINAL PAGE IS  
OF POOR QUALITY

XXXXXXXXXX XXX

|                | LEAD  | TRAIL | PEAK  | AREA    | SHAPE  | ORDER |
|----------------|-------|-------|-------|---------|--------|-------|
| PARTICLE NO. 1 | 1.900 | 1.200 | 1.600 | 71.900  | RANDOM | 5     |
| PARTICLE NO. 2 | 2.200 | 1.450 | 1.950 | 47.400  | RANDOM | 5     |
| PARTICLE NO. 3 | 2.750 | 1.900 | 2.400 | 100.000 | RANDOM | 5     |

POTENTIAL GRADIENT = 10.6VOLTS/CM  
UCS = -.20MICRON CM/VOLT SEC

THETA = .31CM  
SAMPLE RADIUS = .750

WALL TEMPERATURE = 308.0000DEGREES K  
CENTER TEMPERATURE = 310.0000DEGREES K

ORIGINAL PAGE IS  
OF POOR QUALITY

07/21/77 SCOPE 3.4.4 L420 LEHIGH U. 07/11/77

10.45.34.OPTIC4R FROM

10.45.34.OPTIC,3\*\*\*\*,T15,\*KRUMP.

10.45.35.ACCOUNT(\*\*\*)

10.45.35.PFL(50000)

10.45.35.MAP(PART)

10.45.35.PAGES(N,20)

10.45.35.PUN(S)

10.45.45. 40000 OCTAL REQUIRED

10.45.46. 6.629 CP SECONDS COMPILE

10.45.46.LGO.

10.46.03. 31204 PLOTTER FUNCTION UNITS USED

10.46.03.EXIT

10.46.03.OP 00001792 WORDS - FILE PLOT , DC 30

10.46.03.OP 00003520 WORDS - FILE OUTPUT , DC 40

10.46.03.SYSTEM SECONDS USED BY THIS JOB = 8.1

10.46.03.EXECUTION COST OF THIS JOB, NOT INCL I/O COST, IS \$ 1.13

10.46.03.CURRENT AUTHORIZATION BALANCE IS \$ 430.94

10.46.03.NR. OF NON-STANDARD (DISK) CIO CALLS = 32

10.46.03.NR. OF SYSTEM REQUESTS = 226

10.46.03.MAXIMUM 44000 CM WORDS USED.

10.46.03.OP 20.296 SEC.

10.46.03.OP 3.095 SEC.

10.46.03.CH .905 SEC.

\*\*\*\*\* 10.47.57. OPTIC4R 000798 LINES PRINTED /// END OF LIST /// LQ 23

\*\*\*\*\* 10.47.57. OPTIC4R 000798 LINES PRINTED /// END OF LIST /// LQ 23

ORIGINAL PAGE IS  
OF POOR QUALITY